

## Diffusion of cosmic rays in MHD turbulence with magnetic mirrors

A. LAZARIAN<sup>1,2</sup> AND SIYAO XU<sup>3</sup>

<sup>1</sup>*Department of Astronomy, University of Wisconsin, 475 North Charter Street, Madison, WI 53706, USA*

<sup>2</sup>*Center for Computation Astrophysics, Flatiron Institute, 162 5th Ave, New York, NY 10010*

<sup>3</sup>*Institute for Advanced Study, 1 Einstein Drive, Princeton, NJ 08540, USA<sup>a</sup>*

### ABSTRACT

As the fundamental physical process with many astrophysical implications, the diffusion of cosmic rays (CRs) is determined by their interaction with magnetohydrodynamic (MHD) turbulence. We consider the magnetic mirroring effect arising from MHD turbulence on the diffusion of CRs. Due to the intrinsic superdiffusion of turbulent magnetic fields, CRs with large pitch angles that undergo mirror reflection, i.e., bouncing CRs, are not trapped between magnetic mirrors, but move diffusively along the turbulent magnetic field, leading to a new type of parallel diffusion, i.e., mirror diffusion. This mirror diffusion is in general slower than the diffusion of non-bouncing CRs with small pitch angles that undergo gyroresonant scattering. The critical pitch angle at the balance between magnetic mirroring and pitch-angle scattering is important for determining the diffusion coefficients of both bouncing and non-bouncing CRs and their scalings with the CR energy. We find non-universal energy scalings of diffusion coefficients, depending on the properties of MHD turbulence.

### 1. INTRODUCTION

Charged energetic particles or cosmic rays (CRs) are an important ingredient in the physical processes in space and astrophysical environments. It is customary to use the term “energetic particles” in space physics. The theoretical understanding on their acceleration and diffusion in the Solar atmosphere, solar wind, Earth magnetosphere, and heliosphere is important for studying the properties of the interplanetary magnetic field, solar modulation of Galactic CRs, and space weather forecasting (Parker 1965; Jokipii 1971; Singer et al. 2001).

The energetic particles with higher energies outside our direct neighborhood, i.e., of Galactic and extragalactic origin, are usually referred to as CRs. The knowledge on the acceleration and diffusion of CRs is essential for probing their sources, explaining their chemical composition, studying their roles in ionizing molecular gas and circumstellar discs (e.g., Schlickeiser et al. 2016; Padovani et al. 2018), driving galactic winds (e.g., Ipavich 1975; Holguin et al. 2019), and feedback heating in clusters of galaxies (e.g., Guo & Oh 2008; Brunetti & Jones 2014), as well as modeling the synchrotron foreground emission for cosmic microwave background (CMB) radiation and redshifted 21 cm radiation (e.g., Cho & Lazarian 2002a; Cho et al. 2012). In this work, we focus on the diffusion physics that is generally applicable to energetic particles of Solar origin and CRs. Thus we do not distinguish between them and will only use the term “CRs”.

The diffusion of CRs is governed by their interaction with turbulent magnetic fields, as well as the magnetic fluctuations arising from the instabilities induced by CRs, i.e., the streaming instability (Kulsrud & Pearce 1969). In this work we focus on the former type of interaction. The CRs interaction with magnetic turbulence has been a subject of intensive research for decades (Jokipii 1966; Kulsrud & Pearce 1969; Schlickeiser & Miller 1998; Giacalone & Jokipii 1999). However, ad hoc models for magnetohydrodynamic (MHD) turbulence were adopted in early studies.<sup>1</sup>

The recently developed theories of MHD turbulence (Goldreich & Sridhar 1995; Lazarian & Vishniac 1999; Lithwick & Goldreich 2001) have been numerically tested (Cho & Vishniac 2000; Maron & Goldreich 2001; Cho et al. 2002; Cho & Lazarian 2003; Beresnyak 2014; Kowal & Lazarian 2010; Kowal et al. 2017, see also the book by Beresnyak & Lazarian 2019), which are also supported by solar wind observations (e.g., Horbury et al. 2008; Luo & Wu 2010; Forman et al. 2011). The development of MHD turbulence theories allows important advances in studying the pitch-angle scattering, stochastic acceleration, spatial diffusion of CRs along the magnetic field (Chandran 2000a; Yan & Lazarian 2002, 2004; Brunetti & Lazarian 2007; Yan & Lazarian 2008; Lynn et al. 2012; Xu & Yan 2013; Xu & Lazarian 2018; Sioulas et al. 2020; Lemoine & Malkov 2020), superdiffusion and diffusion perpendicular to the mean magnetic field (Yan & Lazarian 2008; Lazarian & Yan 2014), propagation

<sup>1</sup> The model of isotropic MHD turbulence (see Schlickeiser 2002) and 2D + slab superposition model of solar wind turbulence (Matthaeus et al. 1990) adopted in early studies are in contradiction with MHD turbulence simulations and are also challenged by solar wind observations (e.g., Horbury et al. 2008).

of CRs in weakly ionized astrophysical media (Xu et al. 2016), and interactions of CRs with relativistic MHD turbulence (Demidem et al. 2020). These studies bring significant changes to the standard diffusion models of CRs based on the ad hoc models of MHD turbulence (e.g., Matthaeus et al. 1990; Kóta & Jokipii 2000; Qin et al. 2002) and shed light on some long-standing problems and observational puzzles (e.g., Palmer 1982; Evoli & Yan 2014; López-Barquero et al. 2016; Krumholz et al. 2020). Naturally, the propagation of CRs should be modeled using the tested MHD turbulence theories in order to explain multifrequency observations and direct CR measurements (e.g., Nava & Gabici 2013; Cohet & Marcowith 2016; Orlando 2018; Gabici et al. 2019; Amato & Casanova 2021; Fornieri et al. 2021). We are still far from fully understanding the diffusion of CRs to interpret the observations near the Earth and in the vicinity of CR sources and their differences. This motivates us to further study the fundamental physics of CR diffusion in this work.

For CRs interacting with magnetic irregularities, in addition to the pitch-angle scattering, it has long been known that the CR propagation can also be affected by magnetic mirror reflection (Fermi 1949; Noerdlinger 1968; Cesarsky & Kulsrud 1973; Klepach & Ptuskin 1995; Chandran 2000b). The magnetic mirroring effect was explored, for instance, for solving the 90° problem of the quasilinear theory (QLT, Jokipii 1966) for pitch-angle scattering. In these early studies, the mirroring effect was invoked for trapping CRs that bounce back and forth between two mirror points, but it has not been considered in the context of the numerically tested modern theories of MHD turbulence.

In MHD turbulence, compressions of magnetic fields, which are generated by pseudo-Alfvén modes in an incompressible medium and slow and fast modes in a compressible medium, naturally give rise to the mirroring effect over a range of length scales following the energy cascade of turbulence. The interaction of CRs with magnetic mirrors is regulated by the dynamics of turbulent magnetic fields. In particular, this work will demonstrate that the intrinsic perpendicular superdiffusion of turbulent magnetic fields (Lazarian & Vishniac 1999; Eyink et al. 2013; Lazarian & Yan 2014) and its interaction with the parallel diffusion should be taken into account when studying the CR diffusion subject to the mirroring effect.

By using the numerically tested scalings of MHD turbulence (Cho & Lazarian 2003), Xu & Lazarian (2020) (hereafter XL20) investigated the scattering of CRs with the mirroring effect included. There we confirmed the dominant role of fast modes in gyroresonant scattering, and we found that the resulting diffusion coefficient can be significantly smaller than that in the absence of magnetic mirroring.

In this work, by taking into account the intrinsic dynamics of MHD turbulence, i.e., magnetic field perpendicular superdiffusion, we investigate the effect of magnetic mirroring on the parallel diffusion of CRs. This new diffusion mechanism arising from the mirroring effect in MHD turbulence should be considered together with other diffusion processes related to scattering and streaming of CRs for a more com-

prehensive description of CR propagation. Here we focus on the fundamental physics of the mirror diffusion mechanism and the formulation of its diffusion coefficient. Its applicability to various astrophysical media and its confrontation with observations will be studied in our future work (see e.g., Xu 2021).

In what follows, in Section 2, we introduce the perpendicular superdiffusion of both turbulent magnetic fields and CRs and its effect on the parallel diffusion of bouncing CRs. In Sections 3 and 4, we formulate the diffusion coefficients of bouncing CRs in compressible and incompressible MHD turbulence, respectively. In Section 5, we consider the exchange between bouncing and non-bouncing CRs and discuss the averaged diffusion coefficient on scales much larger than their mean free paths. Finally, the discussion and the summary of our main results are given in Sections 6 and 7.

## 2. SPATIAL DIFFUSION OF BOUNCING PARTICLES

The mirroring effect in MHD turbulence causes diffusion of CRs along turbulent magnetic fields. This diffusion parallel to the *local* magnetic field, i.e., "parallel diffusion", is affected by the superdiffusion of turbulent magnetic fields in the direction perpendicular to the mean magnetic field. Below we will discuss in detail these two types of diffusion and their relation.

### 2.1. Magnetic mirrors in MHD turbulence

MHD turbulence can be decomposed into Alfvén, slow, and fast modes (Goldreich & Sridhar 1995; Lithwick & Goldreich 2001; Cho & Lazarian 2002b, 2003). Alfvén modes induce magnetic field wandering, which accounts for the superdiffusion of CRs perpendicular to the mean magnetic field (Lazarian & Vishniac 1999; Eyink et al. 2013; Lazarian & Yan 2014). Slow modes are passively mixed by Alfvén modes and have the same anisotropic scaling as Alfvén modes (Lithwick & Goldreich 2001; Cho & Lazarian 2003). Fast modes have an independent energy cascade and isotropic energy distribution (Cho & Lazarian 2002b, 2003; Kowal et al. 2009). Magnetic compressions arising from slow and fast modes can act as magnetic mirrors that result in bouncing of particle among the mirror points. Their detailed statistical properties are presented in Appendix.

The magnetic mirroring effect caused by static magnetic bottles is well known in plasma physics (e.g., Post 1958; Budker 1959; Noerdlinger 1968; Kulsrud & Pearce 1969). A particle with the Larmor radius smaller than the variation scale of the magnetic field preserves its adiabatic invariant, i.e.  $p_{\perp}^2/B = \text{const}$ . It implies

$$\frac{p_{\perp}^2}{B_0} = \frac{p^2}{B_0 + \delta b} \quad (1)$$

for the condition of magnetic mirroring, where  $B_0$  and  $B_0 + \delta b$  are the magnetic field strengths in the weak and strong magnetic field regions, and  $p$  is the total momentum of the particle. As the total momentum is preserved, it is easy to see that the particles with  $\mu < \mu_{lc}$ , where  $\mu$  is the pitch-angle

cosine and  $\mu_{lc}$  satisfies

$$\mu_{lc}^2 = \cos^2 \theta_{lc} = \frac{\delta b}{B_0 + \delta b}, \quad (2)$$

are subject to magnetic mirroring. Here  $\theta_{lc}$  is angular size of the loss cone for escaping particles with smaller pitch angles. For slow and fast modes in MHD turbulence with a spectrum of magnetic fluctuations, there is  $\delta b = b_k$ . When  $b_k$  at wavenumber  $k$  is significantly smaller than the mean magnetic field strength  $B_0$ , the above expression can be approximated by

$$\mu_{lc}^2 \approx \frac{b_k}{B_0}. \quad (3)$$

The amplitude of  $b_k$  depends on the driven magnetic perturbations  $\delta B_s$  and  $\delta B_f$  of slow and fast modes. Their relation depends on the compressibility of the medium and plasma  $\beta$ , where  $\beta = P_{\text{gas}}/P_{\text{mag}} > 1$ , and  $P_{\text{gas}}$  and  $P_{\text{mag}}$  are gas/plasma and magnetic pressures. In a in high- $\beta$  medium, with the sonic Mach number  $M_s = V_L/c_s < 1$ , where  $V_L$  is the driven turbulent velocity,  $c_s$  is the sound speed,  $\delta B_s$  is expected to be larger than  $\delta B_f$ . In the opposite limit of magnetically dominated medium with  $\beta < 1$ , there is  $\delta B_s < \delta B_f$ .

In the literature, particles with  $\mu < \mu_{lc}$  are considered “trapped” in magnetic bottles and thus they cannot diffuse. However, as we will show below (Section 2.3), this is an erroneous notion. In fact, for 3D propagation in MHD turbulence, magnetic mirroring results in a new type of parallel diffusion of bouncing particles.

## 2.2. Perpendicular superdiffusion

CRs following magnetic field lines<sup>2</sup> undergo pitch-angle scattering via the interaction with small-scale magnetic fluctuations and bouncing among magnetic mirrors (see above). In the meantime, the dispersion of their trajectories in the direction perpendicular to the mean magnetic field is determined by the dispersion of magnetic field lines. This dispersion increases with the propagation distance of CRs along the magnetic field and accounts for the perpendicular diffusion of CRs, as pointed out by Jokipii (1966). The superdiffusive nature of this dispersion within the range of length scales of strong MHD turbulence was later found by Lazarian & Vishniac (1999) when they analytically quantified the magnetic field wandering induced by the Alfvénic component<sup>3</sup> of MHD turbulence for both super-Alfvénic ( $M_A = V_L/V_A > 1$ ) and sub-Alfvénic ( $M_A < 1$ ) turbulence, where  $V_A$  is the Alfvén speed. We note that the perpendicular superdiffusion is with respect to the mean magnetic field in sub- and trans-Alfvénic ( $M_A = 1$ ) turbulence, and with respect to the local mean field, i.e., the magnetic field averaged over scales

less than  $l_A = LM_A^{-3}$  in super-Alfvénic turbulence (Lazarian 2006), where  $L$  is the turbulence driving scale, and  $l_A$  is the scale where the local turbulent velocity becomes equal to  $V_A$ . For the turbulent motions on scales larger than  $l_A$ , the effect of magnetic field is subdominant, and they gradually get isotropic, similar to the hydrodynamic Kolmogorov turbulence.

For sub-Alfvénic turbulence, there exists a scale  $l_{\text{tran}} = LM_A^2$  for the transition from the weak turbulence over the scales  $[l_{\text{tran}}, L]$  to the strong turbulence on smaller length scales. In the weak turbulence regime, the magnetic fields exhibit normal diffusion, i.e. the mean squared separation between magnetic field lines increases with  $s$ , where  $s$  is the distance measured along the magnetic field lines (Lazarian & Vishniac 1999).

We next consider the divergence of magnetic field lines over scales less than  $l_{\text{tran}}$ . Naturally, when one follows the magnetic field line over the parallel scale  $l_{\parallel}$  of a turbulent eddy, the magnetic field line has its perpendicular displacement equal to the transverse size  $l_{\perp}$  of the eddy. As  $l_{\perp}$  can be both positive and negative, the dispersion  $\langle y^2 \rangle$  of magnetic field lines increases as

$$d\langle y^2 \rangle \approx l_{\perp}^2 \frac{ds}{l_{\parallel}}, \quad (4)$$

where  $ds$  is the distance measured along the magnetic field line, and the bracket denotes an ensemble average. Using the above relation and the scaling relation between  $l_{\parallel}$  and  $l_{\perp}$  for sub-Alfvénic turbulence (Lazarian & Vishniac (1999), see also Appendix A), one can find

$$d\langle y^2 \rangle \approx \langle y^2 \rangle^{2/3} M_A^{4/3} L^{-1/3} ds. \quad (5)$$

If the expression on the right-hand side were “constant  $\times ds$ ”, Eq. (5) would describe the random walk of field lines. However, it has a power-law dependence on the field line separation with a positive power index, i.e.  $\propto \langle y^2 \rangle^{2/3}$ , leading to an accelerating superdiffusion as magnetic field lines spread out. The numerical demonstration of the superdiffusion of turbulent magnetic fields can be found in, e.g., Lazarian et al. (2004); Beresnyak (2013).

The physical explanation of the effect is the following. As we follow the magnetic field line the distance  $\sim s$ , the divergence rate of field lines increases with larger and larger turbulent eddies contributing to the dispersion of field line separations. A similar effect in hydrodynamic turbulence is related to the accelerated separation of a pair of test particles with time, which is known as Richardson dispersion (Richardson 1926).<sup>4</sup> The accelerated divergence of magnetic field lines results in the superdiffusive field line separations. The analogy between the Richardson dispersion and the superdiffusion of magnetic fields introduced in Lazarian & Vishniac (1999) was discussed in detail in Eyink et al. (2011).

<sup>2</sup> In the presence of turbulence, CRs follow the magnetic flux tubes averaged within their gyro-orbit. We nevertheless adopt the generally accepted way to describe magnetic fields as “magnetic field lines”.

<sup>3</sup> The separation of MHD turbulence into Alfvénic, slow and fast modes was demonstrated numerically in Cho & Lazarian (2002, 2003). The dominance of Alfvénic modes in terms of inducing magnetic field wandering was shown analytically in Lazarian & Vishniac (1999).

<sup>4</sup>

In the presence of magnetic field, this results in the Richardson dispersion of magnetic field lines with time (Eyink et al. 2011, 2013), as a time-dependent analog of the superdiffusion of magnetic field lines in space.

Eq. (5) also applies to the dispersion of separations of CRs that follow magnetic field lines. The resulting superdiffusive perpendicular divergence of CR trajectories was studied in Yan & Lazarian (2008); Lazarian & Yan (2014) in two regimes, one describing the ballistic motion of CRs along the magnetic field, the other describing the diffusion of CRs along the magnetic field. Both regimes were numerically tested in Xu & Yan (2013). For the ballistic propagation, the corresponding dispersion of separations of particles in the perpendicular direction is

$$\langle y^2 \rangle \sim l_{\perp}^2 \approx \frac{s^3}{L} M_A^4, \quad M_A < 1, \quad s < \lambda_{\parallel}, \quad s < L. \quad (6)$$

Here  $s$  is the distance of particles measured along the magnetic field line, and  $\lambda_{\parallel}$  is the CR parallel mean free path.  $y$  can be identified with the displacement of particles perpendicular to the mean magnetic field. Note that the dependence  $\langle y^2 \rangle \propto s^3$  in the above expression is also applicable to super-Alfvénic turbulence at scales less than  $l_A$ , i.e.,  $s < l_A$ .

In the presence of the parallel diffusion, i.e. over the distance  $s > \lambda_{\parallel}$ , the perpendicular dispersion of CRs is modified to scale as  $\langle y^2 \rangle \propto s^{3/2}$ . Naturally, this is still in a superdiffusion regime that arises from the superdiffusive magnetic field line dispersion. Therefore, in strong MHD turbulence, i.e., on scales smaller than  $l_A$  in super-Alfvénic turbulence and  $l_{\text{tran}}$  in sub-Alfvénic turbulence, for both ballistic and diffusive CR propagation along the turbulent magnetic field, CR trajectories get separated superdiffusively in the direction perpendicular to the mean magnetic field, although the law of superdiffusion differs in the two cases. A detailed discussion on the perpendicular (super)diffusion of CRs in different turbulence regimes is provided in Lazarian & Yan (2014) (see Table 1 in Lazarian & Yan 2019).

We note that the concept of perpendicular superdiffusion of CRs contradicts to some existing views of CR transport, e.g. the Non-Linear Guiding Center Theory (NLGCT) (Matthaeus et al. 2003) that is formulated using the 2D/slab model of MHD turbulence. As the (super)diffusion behavior of CRs strongly depends on the properties of MHD turbulence, CR (super)diffusion should be studied using the tested model of MHD turbulence, instead of synthetic models.

### 2.3. Parallel mirror diffusion

The effect of magnetic mirrors on trapping particles was extensively studied in the literature (e.g., Noerdlinger 1968; Kulsrud & Pearce 1969; Cesarsky & Kulsrud 1973). There it was assumed that the trapped particles undergo oscillatory motions between two mirror points of a magnetic bottle, without cumulative diffusion along the magnetic field. As the main difference between this work and earlier studies, here we consider the existence of Alfvénic component of turbulence and the resulting perpendicular superdiffusion of magnetic fields and CRs. As we explain below, in the presence of Alfvénic turbulence, the superdiffusion of magnetic fields does not allow the particles to be trapped in the same magnetic bottle.

For every crossing of a magnetic bottle induced by the compressive component of MHD turbulence with a size  $s$ , the particle experiences perpendicular superdiffusion with the perpendicular displacement  $y$  given in Section 2.2. As a result, the particle escapes the magnetic bottle within one crossing time and then encounters another magnetic bottle within a perpendicular distance  $y$  from the previous magnetic bottle. As a result, the bouncing with the mirror points of different magnetic bottles leads to the diffusive motion of particles along turbulent magnetic field lines. We term this diffusion parallel to local magnetic field arising from the mirroring effect as “parallel mirror diffusion” to distinguish it from the traditional CR parallel diffusion associated with the resonance scattering (see Schlickeiser 2002). We illustrate the parallel mirror diffusion in Fig. 1. CRs that follow diffusing magnetic field lines are not trapped, but move diffusively parallel to the turbulent magnetic field when bouncing with different magnetic mirrors. Through this paper, “bouncing” and “mirroring” are equivalent.

Due to the 3D character of CR motions and the complexity of magnetic field structure at different  $M_A$ , it is important to clarify that the parallel diffusion of CRs in MHD turbulence is the diffusion with respect to the local magnetic field sampled by CRs. At  $M_A < 1$ , the local magnetic field has the direction close to that of the global mean magnetic field, while at  $M_A > 1$ , the magnetic field direction changes significantly on scales larger than  $l_A$ . In the latter case, we consider the parallel mirror diffusion on scales smaller than  $l_A$ . The parallel mirror diffusion of CRs is accompanied by the dispersion of their trajectories in the direction perpendicular to the mean magnetic field (see Fig. 1). The perpendicular superdiffusion of CRs can be observed when their initial separations in space are small, as shown in simulations (Xu & Yan 2013). The exact scaling relation between  $\langle y^2 \rangle$  and  $s$  depends on  $\lambda_{\parallel}$  of bouncing CRs (Section 2.2).  $\lambda_{\parallel}$  is related to the parallel diffusion coefficient  $D_{\parallel}$  by  $D_{\parallel} = 1/3v\lambda_{\parallel}$ , where  $v$  is particle velocity.  $D_{\parallel}$  of bouncing CRs will be derived in the next sections.

## 3. PARALLEL DIFFUSION OF BOUNCING PARTICLES INDUCED BY FAST MODES IN COMPRESSIBLE MHD TURBULENCE

### 3.1. Bouncing and non-bouncing particles

In compressible MHD turbulence, if fast modes carry a significant fraction of the injected turbulent energy, they act as the main agent for scattering particles (Yan & Lazarian 2002, 2004). More recently, XL20 identified the important role of fast modes in both bouncing and scattering CRs. XL20 studied the parallel diffusion associated with the gyroresonant scattering of non-bouncing particles. Here we will focus on the parallel mirror diffusion of bouncing particles.

The scattering causes diffusion in pitch angle. In the quasi-linear approximation (Jokipii 1966), for the gyroresonant scattering by fast modes, the pitch-angle diffusion coefficient

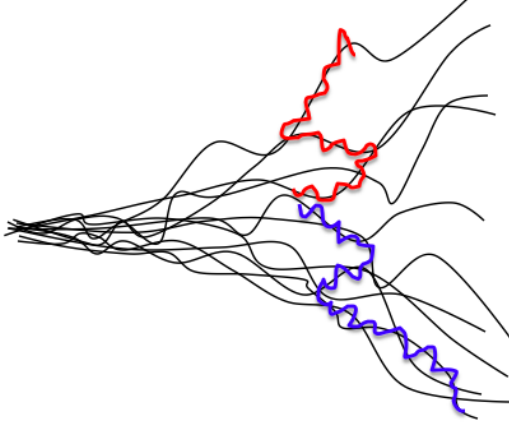


**Figure 1.** Because of the perpendicular superdiffusion of particles following turbulent magnetic field lines, particles that undergo bouncing move diffusively along the local magnetic field. Thin lines represent magnetic field lines. Thick lines represent the trajectories of two particles whose initial separation is small.

is (Voelk 1975)

$$D_{\mu\mu, \text{QLT}, f} = C_{\mu} \int d^3k \frac{k_{\parallel}^2}{k^2} [J_1'(x)]^2 I_f(k) R(k). \quad (7)$$

Here

$$C_{\mu} = (1 - \mu^2) \frac{\Omega^2}{B_0^2}, \quad x = \frac{k_{\perp} v_{\perp}}{\Omega} = \frac{k_{\perp}}{r_g^{-1}}, \quad (8)$$

$B_0$  is the mean magnetic field strength,  $v_{\perp}$  is the perpendicular component of  $v$ ,  $\Omega$  is the gyrofrequency,  $r_g$  is the particle gyroradius, and  $k_{\parallel}$  and  $k_{\perp}$  are parallel and perpendicular components of wavenumber  $k$ . Besides,

$$I_f(k) = C_f k^{-\frac{7}{2}} \quad (9)$$

is the energy spectrum of fast modes (Cho & Lazarian 2002b), with

$$C_f = \frac{1}{16\pi} \delta B_f^2 L^{-\frac{1}{2}}, \quad (10)$$

where  $\delta B_f$  is the magnetic perturbation of fast modes at  $L$ , and

$$R = \pi \delta(\omega_k - v_{\parallel} k_{\parallel} + \Omega) \quad (11)$$

is the resonance function for gyroresonance in the quasilinear approximation, where  $\omega_k$  is the wave frequency. We see that when the pitch angle approaches  $90^\circ$ , the above resonance condition cannot be satisfied with a limited range of  $k$  and decreasing magnetic fluctuation amplitude with increasing  $k$ , leading to the  $90^\circ$  problem<sup>5</sup>. For our analytical estimate, we

<sup>5</sup> The vanishing scattering close to  $90^\circ$  and infinite mean free path in the quasi-linear theory is known as the  $90^\circ$  problem (Fisk et al. 1974).

can use the approximate expression of  $D_{\mu\mu, \text{QLT}, f}$  (Xu et al. 2016; Xu & Lazarian 2018)

$$D_{\mu\mu, \text{QLT}, f} \approx \frac{\pi}{56} \frac{\delta B_f^2}{B_0^2} \left( \frac{v}{L\Omega} \right)^{\frac{1}{2}} \Omega (1 - \mu^2) \mu^{\frac{1}{2}}. \quad (12)$$

We define the rate of change in  $\mu$  due to scattering as the scattering rate (XL20),

$$\Gamma_{s, f} = \frac{2D_{\mu\mu, \text{QLT}, f}}{\mu^2} \approx \frac{\pi}{28} \frac{\delta B_f^2}{B_0^2} \left( \frac{v}{L\Omega} \right)^{\frac{1}{2}} \Omega (1 - \mu^2) \mu^{-\frac{3}{2}}. \quad (13)$$

In the presence of the stochastic magnetic mirrors induced by fast modes, the particles that satisfy the bouncing condition (see below) undergo the bouncing motions among different magnetic mirrors as discussed in Section 2.3. For particles with (see Eq. (3))

$$\mu \approx \sqrt{\frac{b_{fk}}{B_0}}, \quad (14)$$

the bouncing is dominated by the magnetic mirrors at  $k$  with the magnetic perturbation  $b_{fk}$  (Cesarsky & Kulsrud 1973), where

$$b_{fk} = \delta B_f (kL)^{-\frac{1}{4}} \quad (15)$$

according to the scaling of isotropic fast modes (Cho & Lazarian 2002b). The rate of the adiabatic change in  $\mu$  due to the spatial variation of magnetic field is (Cesarsky & Kulsrud 1973, XL20)

$$\begin{aligned} \Gamma_{b, f} &= \left| \frac{1}{\mu} \frac{d\mu}{dt} \right| = \frac{v}{2B_0} \frac{1 - \mu^2}{\mu} b_{fk} k \\ &= \frac{v}{2L} \frac{\delta B_f^4}{B_0^4} \frac{1 - \mu^2}{\mu^7} \end{aligned} \quad (16)$$

at  $\mu > \mu_{\text{min}, f}$ , where

$$\mu_{\text{min}, f} = \sqrt{\frac{b_{fk}(r_g)}{B_0}} = \sqrt{\frac{\delta B_f}{B_0}} \left( \frac{r_g}{L} \right)^{\frac{1}{8}}, \quad (17)$$

and  $b_{fk}(r_g)$  is the magnetic perturbation at  $r_g$ . At  $\mu < \mu_{\text{min}, f}$ , the bouncing rate is

$$\begin{aligned} \Gamma_{b, f} &= \frac{v}{2B_0} \frac{1 - \mu^2}{\mu} b_{fk}(r_g) r_g^{-1} \\ &= \frac{v}{2r_g} \frac{\delta B_f}{B_0} \left( \frac{r_g}{L} \right)^{\frac{1}{4}} \frac{1 - \mu^2}{\mu}. \end{aligned} \quad (18)$$

At the balance between scattering and bouncing, i.e.,  $\Gamma_{s, f} = \Gamma_{b, f}$ , one can find the cutoff  $\mu$  (Eqs. (13) and (16),

$$\mu_c \approx \left[ \frac{14}{\pi} \frac{\delta B_f^2}{B_0^2} \left( \frac{v}{L\Omega} \right)^{\frac{1}{2}} \right]^{\frac{2}{11}}, \quad (19)$$

in agreement with the result in XL20. We define the particles with  $\mu < \mu_c$  as ‘‘bouncing particles’’ and those with  $\mu > \mu_c$

as “non-bouncing” particles. Their motions are dominated by bouncing and scattering, respectively. As shown in Fig. 2,  $\mu_c$  increases with the CR energy  $E_{\text{CR}}$  until reaching its maximum value

$$\mu_{c,\text{max}} = \sqrt{\frac{\delta B_f}{B_0 + \delta B_f}}. \quad (20)$$

Here as an illustration, we consider CR protons, the magnetic field strength  $\delta B_f = B_0 = 3\mu\text{G}$ , and  $L = 30$  pc as the driving scale of interstellar turbulence.

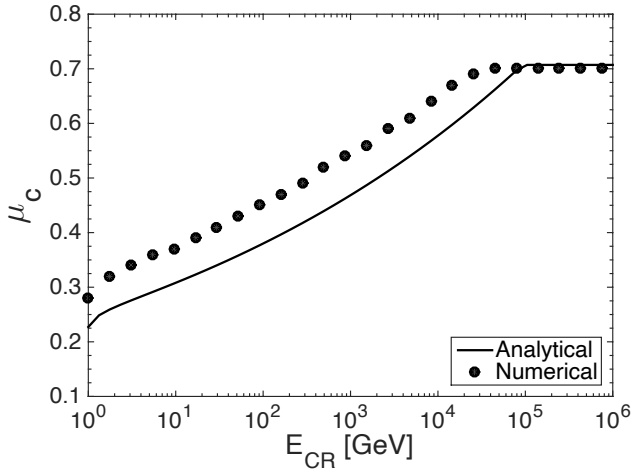


**Figure 2.**  $\mu_c$  as a function of  $E_{\text{CR}}$  for fast modes. The analytical approximation is given by Eq. (19). The numerical result is obtained based on the numerical evaluation of Eq. (7).

### 3.2. Parallel diffusion of bouncing particles

When the mirroring condition  $\mu < \mu_c$  is satisfied, the parallel diffusion of particles with  $\mu$  is regulated by the mirroring effect. Based on the relations in Eqs (14) and (15), bouncing particles diffuse along the magnetic field with a step size

$$k^{-1} = L \left( \frac{\delta B_f}{B_0} \right)^{-4} \mu^8 \quad (21)$$

for  $k^{-1} > r_g$ , or equivalently  $\mu > \mu_{\text{min},f}$ . At  $\mu < \mu_{\text{min},f}$ , the step size of parallel diffusion is  $r_g$ , corresponding to the

Bohm diffusion. The maximal step size of bouncing particles corresponds to  $\mu_c$ ,

$$k_c^{-1} = L \left( \frac{\delta B_f}{B_0} \right)^{-4} \mu_c^8. \quad (22)$$

It decreases with the increase of  $\delta B_f/B_0$  (see Eq. (19)) and should not exceed  $L$ . The bouncing of the particles with  $\mu > \mu_c$  by the magnetic fluctuations on scales larger than  $k_c^{-1}$  is less efficient than their gyroresonant scattering by small-scale magnetic fluctuations.

The corresponding parallel diffusion coefficient arising from bouncing is

$$D_{\parallel,f,b}(\mu) = \begin{cases} v\mu k^{-1} = vL \left( \frac{\delta B_f}{B_0} \right)^{-4} \mu^9, & \mu_{\text{min},f} < \mu < \mu_c, \\ v\mu r_g, & \mu < \mu_{\text{min},f}. \end{cases} \quad (23a)$$

The strong dependence on  $\mu$  comes from the  $\mu$ -dependence of the size of the dominant magnetic mirror field (Eq. (21)). The bouncing makes the parallel diffusion of CRs with a smaller  $\mu$  more inefficient. This is opposite to the expectation from the quasi-linear scattering theory.

We first assume an isotropic pitch angle distribution for a simple analytical estimate of the parallel diffusion coefficient. By integrating  $D_{\parallel,f,b}(\mu)$  over  $\mu$ , we find the parallel diffusion coefficient as a sum of the contributions from the multi-scale magnetic mirror field for bouncing particles with different  $\mu$ ,

$$D_{\parallel,f,b} = \int_0^{\mu_c} D_{\parallel,f,b}(\mu) d\mu \approx \frac{1}{10} vL \left( \frac{\delta B_f}{B_0} \right)^{-4} \mu_c^{10}, \quad (24)$$

where we consider that the contribution from  $D_{\parallel,f,b}(\mu)$  at  $\mu < \mu_{\text{min},f}$  is small.

In the situation with an anisotropic pitch angle distribution resulting from the anisotropic scattering (see Eq. (12)), we focus on the pitch-angle diffusion and use the spatially averaged Fokker-Planck equation

$$\frac{\partial f}{\partial t} = \frac{\partial}{\partial \mu} \left[ D_{\mu\mu} \frac{\partial f}{\partial \mu} \right] \quad (25)$$

to derive the particle distribution function  $f$  under the effect of scattering. If the steady state, i.e.,  $\partial f/\partial t = 0$ , can be reached, we have

$$D_{\mu\mu} \frac{df}{d\mu} = C, \quad (26)$$

where  $-C$  is the constant flux of particles in  $\mu$  space. The steady-state solution is

$$f(\mu) = -C \int_{\mu}^{\mu_c} \frac{d\mu'}{D_{\mu\mu}(\mu')} + f(\mu_c). \quad (27)$$

To simplify the evaluation of  $f(\mu)$ , we further adopt the boundary condition

$$f(\mu_c) = 0 \quad (28)$$

by assuming that the diffusion of non-bouncing particles is relatively fast and the non-bouncing particles at  $\mu > \mu_c$  instantly escape from the system. This assumption implies that the diffusion coefficient of the non-bouncing particles is much larger than that of the bouncing particles. Its validity will be examined later. We then normalize the distribution function of the bouncing particles

$$f' = \frac{f}{\int_0^{\mu_c} f d\mu} \quad (29)$$

to have unit integral,

$$\int_0^{\mu_c} f' d\mu = 1. \quad (30)$$

The parallel diffusion coefficient of bouncing particles under the consideration of anisotropic pitch angle distribution is then

$$D_{\parallel,f,b} = \int_0^{\mu_c} D_{\parallel,f,b}(\mu) f' d\mu, \quad (31)$$

where  $D_{\parallel,f,b}(\mu)$  is given by Eq. (23). It is evident that the above calculation of  $D_{\parallel,f,b}$  for bouncing particles depends on  $D_{\mu\mu}$  that originates from scattering.

To provide an example for illustrating the parallel diffusion of bouncing particles, in Fig. 3, we present the numerically calculated  $D_{\parallel,f,b}$  as a function of  $E_{\text{CR}}$  and its analytical approximation (Eq. (24)). The same parameters as used in Fig. 2 are adopted. We see that the simplification by using an isotropic pitch angle distribution in Eq. (24) does not significantly affect the result. This is because for scattering by fast modes,  $D_{\mu\mu, \text{QLT}, f}$  and the resulting  $f(\mu)$  are not significantly anisotropic.<sup>6</sup> The analytical estimate has the energy dependence as  $D_{\parallel,f,b} \propto E_{\text{CR}}^{10/11}$  for relativistic particles (Eqs. (19) and (24)), which is close to  $D_{\parallel,f,b} \propto E_{\text{CR}}$ . The numerical result is a bit shallower and can be fitted by  $D_{\parallel,f,b} \propto E_{\text{CR}}^{0.7}$ . The discrepancy between the analytical and numerical results at the high-energy end comes from the energy dependence of  $D_{\parallel,f,b}(\mu)$  at  $\mu < \mu_{\text{min},f}$  (Eq. (23)), which is not taken into account in the analytical approximation.

As a comparison, in Fig. 3 we also add the parallel diffusion coefficient of non-bouncing particles determined by the gyroresonant scattering by fast modes derived in XL20. The analytical approximation is given by

$$\begin{aligned} D_{\parallel,f,nb} &= \frac{v^2}{4} \int_{\mu_c}^1 d\mu \frac{(1-\mu^2)^2}{D_{\mu\mu, \text{QLT}, f}(\mu)} \\ &\approx \frac{28}{5\pi} \frac{B_0^2}{\delta B_f^2} \left( \frac{v}{L\Omega} \right)^{-\frac{1}{2}} \frac{v^2}{\Omega} [4 - \sqrt{\mu_c}(5 - \mu_c^2)], \end{aligned} \quad (32)$$

where the lower bound in integration is given by  $\mu_c$  (see Cesarsky & Kulsrud 1973). The resulting  $D_{\parallel,f,nb}$  for non-bouncing particles is shallower than  $\propto E_{\text{CR}}^{0.5}$  except for the

high-energy end with a constant  $\mu_c$ . Its scaling with  $E_{\text{CR}}$  is not an exact power law, but can be approximated by  $\propto E_{\text{CR}}^{1/3}$  (see Fig. 3). We see that there is  $D_{\parallel,f,b} < D_{\parallel,f,nb}$  for all CR energies considered here. This justifies the assumption on the boundary condition in Eq. (28). The bouncing particles have a more inefficient diffusion compared with the non-bouncing particles.

We note that in the above illustration, we assume  $\delta B_f = B_0$ . In this case with  $\delta B_f < B_0$ , both bouncing and non-bouncing particles would have larger diffusion coefficients. Nevertheless, the diffusion of non-bouncing particles is expected to be faster than that of bouncing particles.

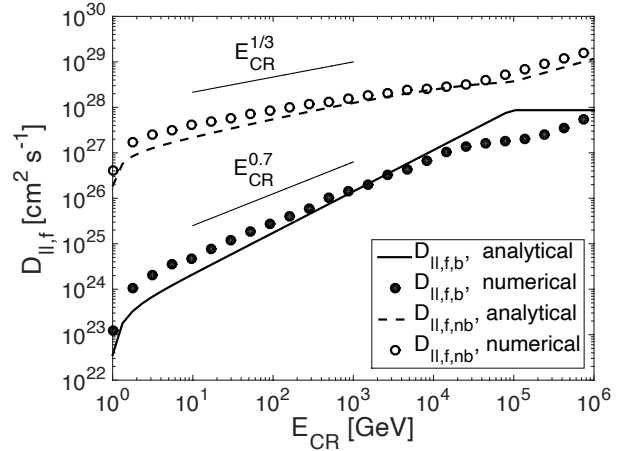


**Figure 3.** Parallel diffusion coefficients  $D_{\parallel,f,b}$  of bouncing CRs and  $D_{\parallel,f,nb}$  of non-bouncing CRs as a function of CR energy in compressible MHD turbulence with fast modes dominating both bouncing and scattering. The analytical approximations are given by Eq. (24) and Eq. (32), respectively.

## 4. PARALLEL DIFFUSION OF BOUNCING PARTICLES IN INCOMPRESSIBLE MHD TURBULENCE

### 4.1. Trans-Alfvénic turbulence

CRs propagation in incompressible MHD turbulence was considered in many earlier studies using isotropic MHD turbulence model or 2D/slab superposition model (Matthaeus et al. 1990). Later it was found that if turbulent energy is injected at large scales, as this is the case of interstellar tur-

<sup>6</sup> The result derived from isotropic pitch angle distribution is supposed to be larger than the one derived from anisotropic distribution. Our analytical approximation underestimates the former due to the underestimation of  $\mu_c$  (see Fig. 2).

bulence (e.g., [Chepurnov et al. 2010](#)), the gyroresonant scattering by both Alfvén modes and pseudo-Alfvén modes is inefficient especially for low-energy CRs due to the scale-dependent anisotropy of MHD turbulence ([Chandran 2000a](#); [Yan & Lazarian 2002](#)). [Yan & Lazarian \(2002\)](#) further argued that fast modes in compressible MHD turbulence, rather than Alfvén modes, determine the scattering of GeV CRs in our galaxy (see [Xu & Lazarian 2018](#) for discussion on importance of slow modes in TTD interaction with CRs). However, considering the variety of astrophysical conditions, there are situations where fast modes are subject to severe damping ([Yan & Lazarian 2004](#); [Brunetti & Lazarian 2007](#); [Xu et al. 2016](#); [Xu & Lazarian 2018](#)). When fast modes are severely damped, or plasma  $\beta$  is large (see Section 2.1), or the injected energy of fast modes is small, additional sources for confining CRs are needed. This motivates us to study CR diffusion in idealized incompressible MHD turbulence or compressible MHD turbulence with a very small energy fraction in fast modes. In this situation, we focus on the mirroring effect induced by pseudo-Alfvén (slow) modes. The magnetic mirroring effect has been found in XL20 to be important for confining CRs in incompressible MHD turbulence. Here we will formulate the corresponding parallel diffusion coefficient.

The pitch-angle diffusion coefficients for gyroresonant interactions with Alfvén and pseudo-Alfvén modes in the quasi-linear approximation are ([Voelk 1975](#)),

$$D_{\mu\mu, \text{QLT}, A} = C_\mu \int d^3k x^{-2} [J_1(x)]^2 I_A(k) R(k), \quad (33)$$

and

$$D_{\mu\mu, \text{QLT}, s} = C_\mu \int d^3k \frac{k_\parallel^2}{k^2} [J_1'(x)]^2 I_s(k) R(k). \quad (34)$$

The magnetic energy spectra are ([Cho et al. 2002](#))

$$I_A(k) = C_A k_\perp^{-\frac{10}{3}} \exp\left(-L^{\frac{1}{3}} \frac{k_\parallel}{k^{\frac{2}{3}}}\right), \quad C_A = \frac{1}{6\pi} \delta B_A^2 L^{-\frac{1}{3}} \quad (35)$$

for Alfvén modes, and

$$I_s(k) = C_s k_\perp^{-\frac{10}{3}} \exp\left(-L^{\frac{1}{3}} \frac{k_\parallel}{k^{\frac{2}{3}}}\right), \quad C_s = \frac{1}{6\pi} \delta B_s^2 L^{-\frac{1}{3}} \quad (36)$$

for pseudo-Alfvén modes, where  $\delta B_A$  and  $\delta B_s$  are their magnetic perturbations at  $L$ . The corresponding scattering rate with contributions from both Alfvén and pseudo-Alfvén modes is

$$\Gamma_{s, \text{inc}} = \frac{2(D_{\mu\mu, \text{QLT}, A} + D_{\mu\mu, \text{QLT}, s})}{\mu^2}. \quad (37)$$

Besides scattering, pseudo-Alfvén modes also generate magnetic mirrors accounting for the bouncing of CRs. The particles with

$$\mu \approx \sqrt{\frac{b_{sk}}{B_0}} \quad (38)$$

mainly undergo the bouncing motion at  $k_\parallel$ , where the magnetic perturbation of pseudo-Alfvén modes is

$$b_{sk} = \delta B_s (k_\perp L)^{-\frac{1}{3}} = \delta B_s (k_\parallel L)^{-\frac{1}{2}} \quad (39)$$

based on the anisotropic scaling of MHD turbulence ([Cho et al. 2002](#)). The bouncing rate is ([Cesarsky & Kulsrud 1973](#), XL20)

$$\begin{aligned} \Gamma_{b,s} &= \left| \frac{1}{\mu} \frac{d\mu}{dt} \right| = \frac{v}{2B_0} \frac{1-\mu^2}{\mu} b_{sk} k_\parallel \\ &= \frac{v}{2L} \aleph_s^2 \frac{1-\mu^2}{\mu^3} \end{aligned} \quad (40)$$

at  $\mu > \mu_{\text{min},s}$ , where

$$\aleph_s = \frac{\delta B_s}{B_0}, \quad (41)$$

$$\mu_{\text{min},s} = \sqrt{\frac{b_{sk}(r_g)}{B_0}} = \sqrt{\aleph_s} \left(\frac{r_g}{L}\right)^{\frac{1}{4}}, \quad (42)$$

and  $b_{sk}(r_g)$  is the magnetic perturbation at  $k_\parallel = 1/r_g$ . At  $\mu < \mu_{\text{min},s}$ , the bouncing rate becomes

$$\begin{aligned} \Gamma_{b,s} &= \frac{v}{2B_0} \frac{1-\mu^2}{\mu} b_{sk}(r_g) r_g^{-1} \\ &= \frac{v}{2r_g} \aleph_s \left(\frac{r_g}{L}\right)^{\frac{1}{2}} \frac{1-\mu^2}{\mu}. \end{aligned} \quad (43)$$

Here we note that as  $\Gamma_{b,s}$  and  $\Gamma_{b,f}$  (Eqs. (16) and (18)) have different  $\mu$  dependence, in the presence of both slow and fast modes in compressible MHD turbulence, the relative importance between the mirroring effects induced by slow and fast modes can change with  $\mu$  (see Section 5.2).

As found in XL20, because of the inefficient scattering by Alfvén and pseudo-Alfvén modes, the effect of magnetic mirrors dominates over the gyroresonant scattering, i.e.  $\Gamma_{b,s} > \Gamma_{s, \text{inc}}$ , for  $\mu < \mu_c$ , and  $\mu_c$  is given by its maximum value<sup>7</sup>

$$\mu_c = \sqrt{\frac{\delta B_s}{B_0 + \delta B_s}}, \quad (44)$$

which is independent of  $E_{\text{CR}}$ .

The non-bouncing particles with  $\mu > \mu_c$  are only poorly constrained by the inefficient scattering, and their diffusion coefficients are expected to be large (see Section 5). For the parallel diffusion of bouncing particles, the step size is

$$k_\parallel^{-1} = L \aleph_s^{-2} \mu^4 \quad (45)$$

at  $\mu > \mu_{\text{min},s}$ , or equivalently,  $k_\parallel^{-1} > r_g$ , and the step size is  $r_g$  at  $\mu < \mu_{\text{min},s}$ . Accordingly, the  $\mu$ -dependent parallel

<sup>7</sup>  $\mu_c$  in incompressible MHD turbulence was approximated to be unity in XL20 for simplicity.

diffusion coefficient is

$$D_{\parallel,\text{inc},b}(\mu) = \begin{cases} v\mu k_{\parallel}^{-1} = vL\aleph_s^{-2}\mu^5, & \mu_{\text{min},s} < \mu < \mu_c, \\ v\mu r_g, & \mu < \mu_{\text{min},s}. \end{cases} \quad (46a)$$

$$(46b)$$

If the pitch angle distribution of bouncing particles is isotropic, then the parallel diffusion coefficient can be approximated by

$$D_{\parallel,\text{inc},b} \approx \int_0^{\mu_c} D_{\parallel,\text{inc},b}(\mu) d\mu = \frac{1}{6} vL\aleph_s^{-2}\mu_c^6, \quad (47)$$

which is energy independent with a constant  $\mu_c$ . Here we neglect the contribution from  $D_{\parallel,\text{inc},b}(\mu)$  at  $\mu < \mu_{\text{min},s}$ .

We next consider the situation with an anisotropic pitch angle distribution. We follow the similar analysis in Section 3.2 to derive  $D_{\parallel,\text{inc},b}$  numerically by using Eqs. (27)-(31). In Eq. (27), we adopt (Eqs. (33) and (34))

$$D_{\mu\mu}(\mu) = D_{\mu\mu,\text{QLT},A} + D_{\mu\mu,\text{QLT},s} \quad (48)$$

to include the gyroresonant scattering by both Alfvén and pseudo-Alfvén modes. Eq. (31) becomes

$$D_{\parallel,\text{inc},b} = \int_0^{\mu_c} D_{\parallel,\text{inc},b}(\mu) f' d\mu, \quad (49)$$

where  $D_{\parallel,\text{inc},b}(\mu)$  is given by Eq. (46).

In Fig. 4, we illustrate the numerically calculated  $D_{\parallel,\text{inc},b}$  with an anisotropic pitch angle distribution in comparison with the analytical approximation with an isotropic pitch angle distribution (Eq. (47)). The same parameters as in Fig. 2 are used, and the turbulence is considered to be trans-Alfvénic with  $\delta B_A = B_0$ . Here we also use  $\delta B_s = B_0$ , i.e.,  $\aleph_s = 1$ . We see that the anisotropic distribution leads to a significantly smaller  $D_{\parallel,\text{inc},b}$  than that derived from an isotropic distribution. Fig. 5(a) displays the anisotropic  $f'$  caused by the anisotropic pitch-angle scattering for different CR energies. The highly anisotropic scattering originates from the scale-dependent anisotropy of Alfvén and pseudo-Alfvén modes. At a small  $\mu$ , the gyroresonance with many uncorrelated eddies with the perpendicular eddy size much smaller than  $r_g$  makes the scattering inefficient (Chandran 2000a; Yan & Lazarian 2002). Consequently, most particles are concentrated at a small  $\mu$ .

The more pronounced anisotropy of  $f'$  for low-energy CRs is caused by the inner cutoff at  $k_{\text{max}}$  of turbulent energy spectrum. XL20 found that for the gyroresonance with Alfvén and pseudo-Alfvén modes, the magnetic fluctuations at

$$k_{\perp p} = \left( \frac{L^{\frac{1}{3}} k_{\parallel,\text{res}}}{8} \right)^{\frac{3}{2}} = 8^{-\frac{3}{2}} k_{\perp,\text{res}} \quad (50)$$

play a dominant role in determining the scattering efficiency. Here the parallel and perpendicular resonant wavenumbers are  $k_{\parallel,\text{res}} \approx \Omega/v_{\parallel}$  and  $k_{\perp,\text{res}} = L^{\frac{1}{2}} k_{\parallel,\text{res}}^{\frac{3}{2}}$  for trans-Alfvénic turbulence. The former is derived from the resonance condition in Eq. (11). When  $k_{\perp p} > k_{\text{max}}$  at a small  $\mu$  and a low

$E_{\text{CR}}$ , the scattering becomes ineffective, leading to a more anisotropic  $f'$ . As a result, the integral in Eq. (49) is dominated by  $D_{\parallel,\text{inc},b}(\mu)$  at a small  $\mu$  (Eq. (46b)) (see Fig. 5(c)). For the parameters adopted here, the CR energy corresponding to  $k_{\perp p} = k_{\text{max}} = 10^{-8} \text{ cm}^{-1}$  and the minimum  $\mu = 0.01$  is indicated by the dashed line in Fig. 4, below which the damping of turbulent spectrum has a significant effect on the diffusion of bouncing particles. The enhanced anisotropy due to damping gives rise to more suppressed diffusion.

At higher energies, Eq. (49) is dominated by  $D_{\parallel,\text{inc},b}(\mu)$  at a larger  $\mu$ , where both  $f'$  and  $D_{\parallel,\text{inc},b}(\mu)$  remain unchanged (Figs. 5(a) and 5(b)), and the resulting  $D_{\parallel,\text{inc},b}$  becomes energy independent (Fig. 4). For high-energy CRs, Eq. (49) is again dominated by  $D_{\parallel,\text{inc},b}(\mu)$  at a small  $\mu$  similar to low-energy CRs, but due to the increase of  $r_g$  with  $E_{\text{CR}}$  (Eq. (46b)). At both low- and high-energy ends,  $D_{\parallel,\text{inc},b}$  has the energy dependence close to  $D_{\parallel,\text{inc},b} \propto E_{\text{CR}}$  as dictated by Eq. (46b).

In the vicinity of a CR source, the initial pitch angle distribution of the injected CRs is important for determining the parallel diffusion of bouncing CRs until they lose the memory about the initial distribution via scattering. Therefore, the CRs closer to the source can have slower diffusion. We note that the pitch angle distribution of low-energy CRs can also be affected by CR-driven instabilities especially near CR sources. Intensive scattering by Alfvén waves generated by streaming CRs can reduce the anisotropy in pitch angle distribution. This effect should be taken into account for more realistic modeling of the parallel diffusion coefficient of low-energy CRs (see, e.g., Blasi et al. 2012).

We see that even though the pitch-angle scattering is inefficient in incompressible trans-Alfvén MHD turbulence, the mirroring effect due to the presence of pseudo-Alfvén modes significantly suppresses the parallel diffusion of CRs.

#### 4.2. Super- and sub-Alfvénic turbulence

In the above analysis, we discussed the case of trans-Alfvénic turbulence with  $M_A = 1$ , or equivalently,  $\delta B_A = B_0$ . Our analysis can be generalized for both super- and sub-Alfvénic turbulence.

For super-Alfvénic turbulence ( $M_A > 1$ ), the perpendicular superdiffusion (Lazarian & Vishniac 1999; Yan & Lazarian 2008; Lazarian 2006; Lazarian & Yan 2014) takes place on scales less than  $l_A$ .<sup>8</sup> For the analysis in Section 4.1 for anisotropic MHD turbulence to be applicable, we use  $l_A$  (Eq. (A4)) as the effective injection scale of turbulence with the injected turbulent velocity equal to  $V_A$ . Therefore, after replacing  $L$  by  $l_A$ , we can still use the expressions in Section 4.1 for describing the parallel diffusion of bouncing particles on scales smaller than  $l_A$  in super-Alfvénic turbulence. We note that  $\delta B_s$  in this case should be measured at  $l_A$  instead of  $L$ .

<sup>8</sup> On scales larger than  $l_A$ , CRs following magnetic field lines undergo isotropic diffusion with the step size equal to  $l_A$  (see Brunetti & Lazarian 2007).

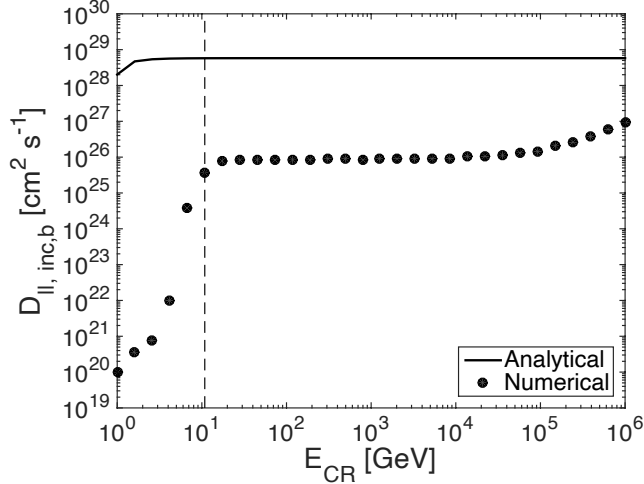


**Figure 4.** Parallel diffusion coefficient  $D_{\parallel, \text{inc}, b}$  of bouncing CRs as a function of CR energy in incompressible MHD turbulence. The numerical and analytical (Eq. (47)) results are obtained using anisotropic and isotropic pitch angle distribution, respectively. The dashed line indicates the energy, below which the diffusion is affected by damping of turbulence.

In sub-Alfvénic turbulence with  $M_A < 1$ , as we discuss in Appendix A, the so-called weak turbulence (Lazarian & Vishniac 1999; Galtier et al. 2000) exists on scales from  $L$  down to  $l_{\text{tran}}$ . Strong MHD turbulence is only developed on scales below  $l_{\text{tran}}$ . In the strong turbulence regime in sub-Alfvénic turbulence, the turbulence scaling is different from that in trans-Alfvénic turbulence, and the turbulent eddies are more elongated, with the elongation depending on  $M_A$  (Lazarian & Vishniac 1999). We notice in Appendix A, if we introduce an effective injection scale  $L_{\text{eff}}$  for sub-Alfvénic turbulence that is given by Eq. (A9), then we can describe the sub-Alfvénic turbulence at scales less than  $l_{\text{tran}}$  as arising from the fictitious driving with the injection scale  $L_{\text{eff}}$  and injection velocity  $V_A$ .  $L_{\text{eff}}$  is larger than the actual injection scale  $L$  by a factor of  $M_A^{-4}$ . Unlike  $l_A$  in super-Alfvénic turbulence, where the transition from isotropic to anisotropic turbulence occurs,  $L_{\text{eff}}$  does not have a well-defined physical meaning. Its introduction, nevertheless, allows us to generalize the results for trans-Alfvénic turbulence to the strong turbulence regime of sub-Alfvénic turbulence by replacing  $L$

used in Section 4.1 by  $L_{\text{eff}}$ .  $\delta B_s$  in this case should be measured at  $L_{\text{eff}}$ , and it is related to the magnetic perturbation  $\delta B_{s, L}$  of pseudo-Alfvén modes at  $L$  by

$$\delta B_s = \delta B_{s, L} M_A^{-2}. \quad (51)$$

In Table 1, we summarize the parameters introduced for generalizing the results on diffusion of bouncing particles in trans-Alfvénic turbulence to super- and sub-Alfvénic turbulence.

## 5. AVERAGED PARALLEL DIFFUSION COEFFICIENTS ON SCALES $\gg \lambda_{\parallel}$

The analysis on the parallel diffusion of bouncing particles in Sections 3 and 4 can be applied to the bouncing CRs near a CR source. On scales much larger than  $\lambda_{\parallel}$  of both bouncing and non-bouncing particles, we need to consider their exchange and the isotropization of pitch angle distribution due to scattering. In this case we define an averaged parallel diffusion coefficient for all particles as

$$D_{\parallel, \text{tot}} \approx \alpha D_{\parallel, b} + (1 - \alpha) D_{\parallel, nb}, \quad (52)$$

where

$$\alpha = \frac{\tau_b}{\tau_b + \tau_{nb}}, \quad 1 - \alpha = \frac{\tau_{nb}}{\tau_b + \tau_{nb}}, \quad (53)$$

$\tau_b$  and  $\tau_{nb}$  represent the times for particles to stay in the bouncing state and non-bouncing state, respectively. As a simple estimate, we have

$$\tau_b \approx \frac{\mu_c^2}{D_{\mu\mu}}, \quad \tau_{nb} \approx \frac{1 - \mu_c^2}{D_{\mu\mu}} \quad (54)$$

to account for the diffusion in pitch angle by scattering and the resulting transition from bouncing (non-bouncing) to non-bouncing (bouncing) particles. For the weakly anisotropic pitch angle distribution under consideration, we can use  $D_{\mu\mu}$  at  $\mu_c$  in the above expression as an approximation. Therefore, Eq. (52) can be rewritten as

$$D_{\parallel, \text{tot}} \approx \mu_c^2 D_{\parallel, b} + (1 - \mu_c^2) D_{\parallel, nb}. \quad (55)$$

Over a timescale  $T$  much longer than  $\tau_b$  and  $\tau_{nb}$ , the mean squared displacement of CRs in the bouncing state is

$$\Delta_b^2 = D_{\parallel, b} \alpha T, \quad (56)$$

and the mean squared displacement of CRs in the non-bouncing state is

$$\Delta_{nb}^2 = D_{\parallel, nb} (1 - \alpha) T. \quad (57)$$

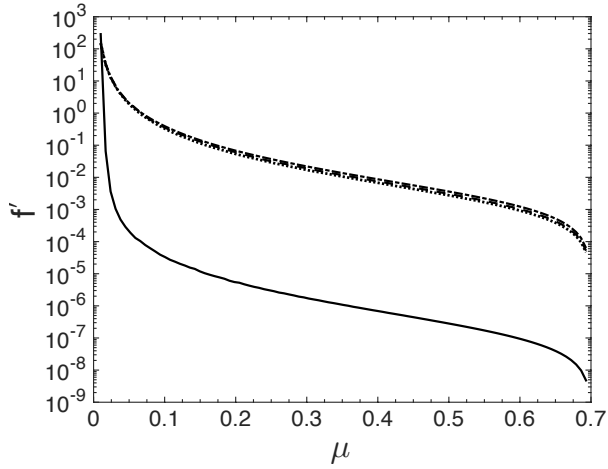
The total mean squared displacement  $\Delta_{\text{tot}}^2 = \Delta_b^2 + \Delta_{nb}^2$  during  $T$  corresponds to a total diffusion coefficient

$$D_{\parallel, \text{tot}} = \frac{\Delta_{\text{tot}}^2}{T} \approx \alpha D_{\parallel, b} + (1 - \alpha) D_{\parallel, nb}, \quad (58)$$

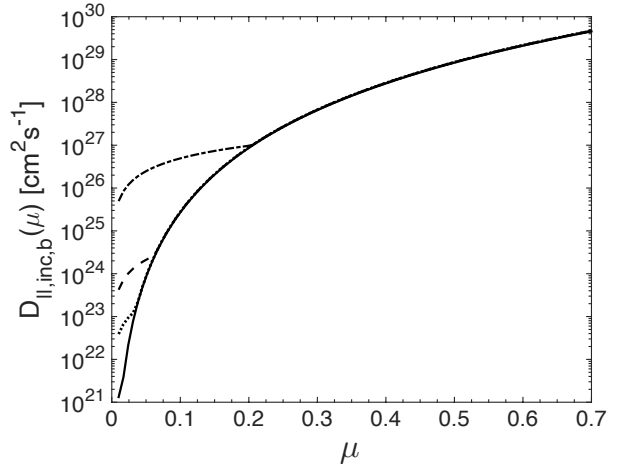
which recovers Eq. (52). In the case with  $D_{\parallel, b} \ll D_{\parallel, nb}$ ,  $D_{\parallel, \text{tot}}$  can be dominated by the diffusion of non-bouncing particles, that is,

$$D_{\parallel, \text{tot}} \approx (1 - \alpha) D_{\parallel, nb}. \quad (59)$$

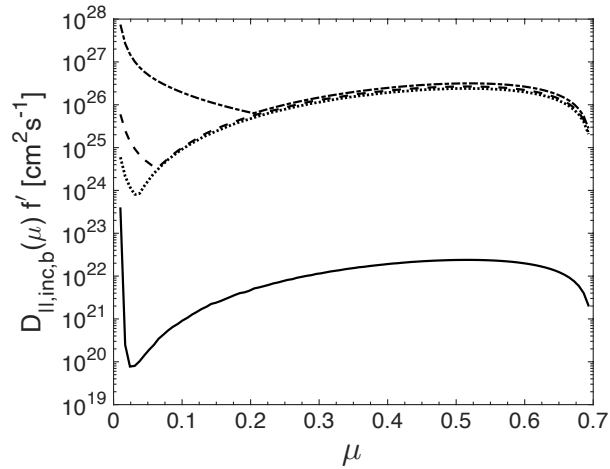
It is different from the parallel diffusion coefficient in XL20 by a factor of  $1 - \alpha$ .



(a)



(b)



(c)

**Figure 5.** (a) Normalized particle distribution function  $f'$ , (b)  $\mu$ -dependent parallel diffusion coefficient  $D_{\parallel,inc,b}(\mu)$ , and (c)  $D_{\parallel,inc,b}(\mu)f'$  vs.  $\mu$  for 4 GeV (solid line),  $10^2$  GeV (dotted line),  $10^3$  GeV (dashed line), and  $10^5$  GeV (dash-dotted line) bouncing CRs in incompressible MHD turbulence.

]

**Table 1.** [

	$L_{\text{eff}}$	$\delta B_s$ at $L_{\text{eff}}$	Range of length scales
Super-Alfvénic turbulence ( $M_A > 1$ )	$l_A = LM_A^{-3}$	$\delta B_s$ at $l_A$	$< l_A$
Sub-Alfvénic turbulence ( $M_A < 1$ )	$LM_A^{-4}$	$\delta B_{s,L} M_A^{-2}$	$< LM_A^2$

### 5.1. Compressible MHD turbulence with fast modes dominating magnetic fluctuations

In Section 3, we derived the parallel diffusion coefficients of bouncing and non-bouncing particles separately (see Fig. 3). Based on these calculations and by using Eq. (55), here we present  $D_{\parallel,f,\text{tot}}$  for all particles interacting with fast modes in compressible MHD turbulence, as shown in Fig. 6. By comparing Fig. 6 with Fig. 3, we see that as  $D_{\parallel,f,nb}$  is considerably larger than  $D_{\parallel,f,b}$  for the range of  $E_{\text{CR}}$  under consideration, the resulting  $D_{\parallel,f,\text{tot}}$  is determined by  $D_{\parallel,f,nb}$  alone and slightly smaller than  $D_{\parallel,f,nb}$  with the increase of  $\mu_c$  toward high energies. We note that unlike  $D_{\parallel,f}$  usually defined for pitch-angle scattering that corresponds to the change of pitch angle by  $90^\circ$ ,  $D_{\parallel,f,nb}$  corresponds to a smaller change of pitch angle and is smaller than  $D_{\parallel,f}$  with  $\mu_c = 0$  (see Eq. (32)).

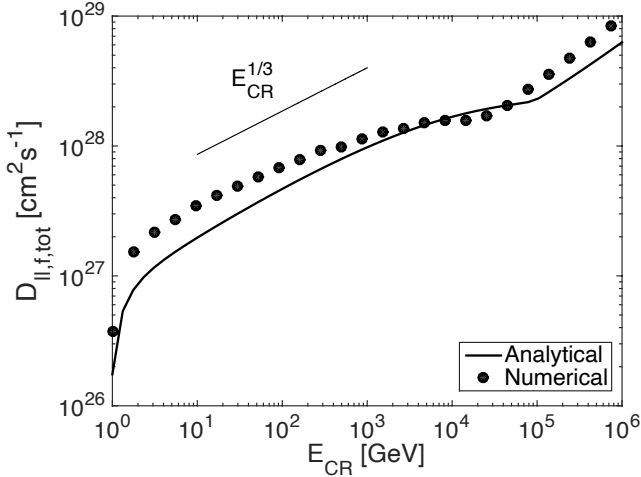


**Figure 6.** Total parallel diffusion coefficient  $D_{\parallel,f,\text{tot}}$  as a function of  $E_{\text{CR}}$  in compressible MHD turbulence with magnetic fluctuations dominated by fast modes.

### 5.2. Compressible MHD turbulence with a varying fraction of fast modes

In realistic astrophysical media, the energy fraction of fast modes depends on the driving condition of turbulence and plasma  $\beta$  (see Section 2.1).

In the presence of both fast and slow modes, the ratio between their bouncing rates (Eqs (16) and (40)) is

$$\frac{\Gamma_{b,f}}{\Gamma_{b,s}} = \frac{\delta B_f^4}{B_0^2 \delta B_s^2} \mu^{-4}, \quad (60)$$

when  $\mu > \mu_{\text{min},f}$  and  $\mu > \mu_{\text{min},s}$ . We use the larger one, i.e.,  $\max[\Gamma_{b,f}, \Gamma_{b,s}]$ , as the bouncing rate. In the case of  $\delta B_f \sim \delta B_s \sim B_0$ , there is always  $\Gamma_{b,f} > \Gamma_{b,s}$  and fast modes dominate bouncing.

As illustrative examples, in Fig. 7, we consider the parallel diffusion coefficients of bouncing and non-bouncing particles in trans-Alfvénic turbulence with a varying fraction of fast modes, and we adopt an isotropic pitch angle distribution.  $\aleph_s$  is fixed at 0.5 to address the role of fast modes in affecting the diffusion coefficients.

(a)  $\delta B_f = 0$ . In the limit case of incompressible MHD turbulence with  $\delta B_f = 0$  (Fig. 7(a)), scattering is inefficient and  $\mu_c$  is given by Eq. (44) (see Fig. 8).  $D_{\parallel,b}$  is consistent with Eq. (47).  $D_{\parallel,nb}$  is

$$D_{\parallel,nb} = \frac{v^2}{4} \int_{\mu_c}^1 d\mu \frac{(1 - \mu^2)^2}{D_{\mu\mu}(\mu)}, \quad (61)$$

where  $D_{\mu\mu}(\mu)$  is given by Eq. (48). As both  $D_{\mu\mu,\text{QLT},A}$  and  $D_{\mu\mu,\text{QLT},s}$  have energy dependence as  $\propto E_{\text{CR}}^{3/2}$  (XL20), the resulting  $D_{\parallel,nb}$  decreases with increasing energy following  $\propto E_{\text{CR}}^{-3/2}$ . Because the turbulence anisotropy is weaker toward larger length scales, higher-energy CRs are more efficiently scattered and have smaller  $D_{\parallel,nb}$ .

(b)  $\delta B_f = 0.01 B_0$ . In compressible MHD turbulence, we consider the scattering rate with contributions from all three modes,

$$\Gamma_{s,\text{tot}} = \frac{2(D_{\mu\mu,\text{QLT},A} + D_{\mu\mu,\text{QLT},s} + D_{\mu\mu,\text{QLT},f})}{\mu^2}. \quad (62)$$

When there is a tiny fraction of fast modes with  $\delta B_f \ll B_0$  (see Fig. 7(b)), the scattering of low-energy CRs is dominated by fast modes despite their small energy fraction. With a constant  $\mu_c$  (Fig. 8),  $D_{\parallel,nb}$  determined by  $D_{\parallel,f,nb}$  increases with energy as  $\propto E_{\text{CR}}^{0.5}$  (see Eq. (32)). The scattering of higher-energy CRs is taken over by Alfvén and slow modes. For bouncing CRs,  $D_{\parallel,b}$  is determined by slow modes and is the same as that in the incompressible turbulence.

(c)  $\delta B_f = 0.1 B_0$ . When we further increase the fraction of fast modes (Fig. 7(c)), scattering is dominated by fast modes for most energies, resulting in the energy dependence of  $\mu_c$  until it reaches its maximum value (Fig. 8). With increasing  $\mu_c$ ,  $D_{\parallel,nb}$  has a weaker dependence on  $E_{\text{CR}}$  than  $\propto E_{\text{CR}}^{0.5}$  (Eq. (32)) for low-energy CRs. For bouncing of CRs, although  $\Gamma_{b,f}$  is larger than  $\Gamma_{b,s}$  at a small  $\mu$  for low-energy CRs (Eq. (60)),  $D_{\parallel,b}$  is still determined by slow modes for most energies and Eq. (47) applies.

(d)  $\delta B_f = 0.5 B_0$ . With a large fraction of fast modes, fast modes dominate both scattering and bouncing.  $D_{\parallel,nb}$  (see Eq. (32)) approximately follows  $\propto E_{\text{CR}}^{1/3}$  (see Fig. 7(d)).  $D_{\parallel,b}$  in this case is given by Eq. (24) and is close to  $\propto E_{\text{CR}}$ .

The thick solid lines in all cases represent the averaged  $D_{\parallel, \text{tot}}$  (Eq. (55)). It is basically determined by  $D_{\parallel, nb}$  as  $D_{\parallel, nb}$  is considerably larger than  $D_{\parallel, b}$ .

Based on the above results, our main findings are:

(i) The difference between  $D_{\parallel, nb}$  dominated by incompressible modes and fast modes comes from not only the different slopes of turbulent energy spectra, but also the anisotropy of turbulence. The scale-dependent turbulence anisotropy in the former case results in a decreasing  $D_{\parallel, nb}$  with increasing  $E_{\text{CR}}$ .

(ii) Even with a small fraction of fast modes, scattering becomes much more efficient than that in incompressible turbulence.

(iii) With an energy-dependent  $\mu_c$ ,  $D_{\parallel, nb}$  dominated by fast modes has a weaker dependence on  $E_{\text{CR}}$  than the case with a constant  $\mu_c$ .

(iv) With a non-zero  $\mu_c$  and a factor  $1 - \alpha$ ,  $D_{\parallel, nb}$  is in general smaller than the parallel diffusion coefficient for gyroresonant scattering with  $\mu_c = 0$  and  $\alpha = 0$ .

(v) The maximum  $D_{\parallel, b}$  depends on the maximum  $\mu_c$ , which is determined by the amplitude of magnetic fluctuations ( $\delta B_s$  or  $\delta B_f$ ) of the modes that dominate bouncing.

(vi) On scales larger than  $\lambda_{\parallel}$  of both bouncing and non-bouncing particles, the averaged parallel diffusion coefficient is determined by that of non-bouncing particles.

(vii) The energy scaling of  $D_{\parallel, \text{tot}}$  is non-universal, depending on the energy fractions of different turbulence modes. In diverse astrophysical environments, the energy fractions of turbulence modes vary with the turbulence parameters, e.g.,  $M_s$ ,  $M_A$  (Cho & Lazarian 2003). For realistic modeling of CR diffusion, prior knowledge of turbulence parameters is necessary, which can be measured with the Gradient Techniques (e.g., Lazarian et al. 2018). This falls beyond the scope of this work and is left to future studies.

## 6. DISCUSSION

### 6.1. Toward a more comprehensive description of CR propagation

Important new findings on CR propagation have been reported over the past two decades. First of all, the fast modes of MHD turbulence were identified as the major scattering agent for diffusion of CRs with  $r_g \ll L$  in the interstellar medium (Yan & Lazarian 2002, 2003). On the contrary, the Alfvén and slow modes, which were traditionally considered for CR diffusion, were found to be very inefficient in scattering (Chandran 2000a; Yan & Lazarian 2002). Therefore, it was believed that, when the CR streaming instability is inefficient, e.g. due to Alfvénic turbulence suppression (see Yan & Lazarian 2002; Farmer & Goldreich 2004; Lazarian 2016), and fast modes are absent, CRs propagate ballistically along magnetic field lines without scattering.<sup>9</sup>

<sup>9</sup> We note that in super-Alfvénic turbulence, CRs that follow the tangled magnetic fields without scattering have an effective mean free path given by  $l_A$  (Brunetti & Lazarian 2007).

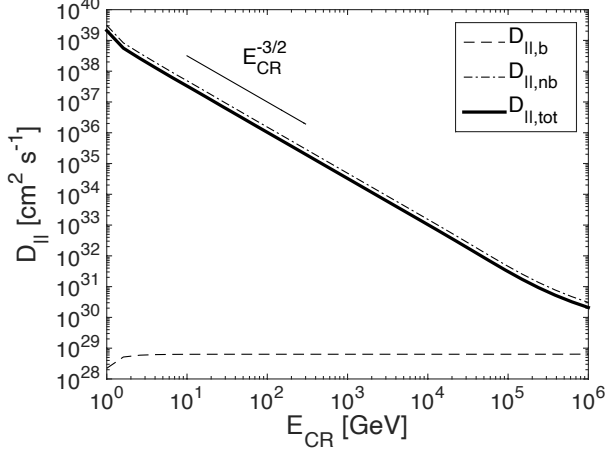
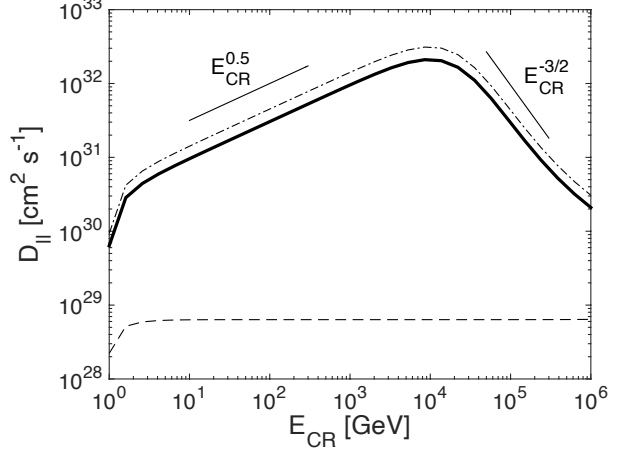
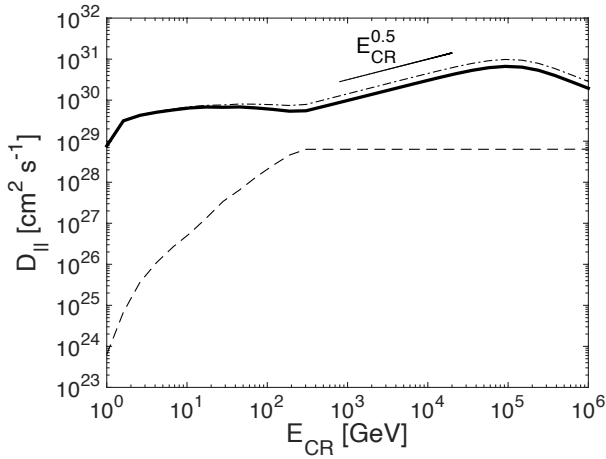
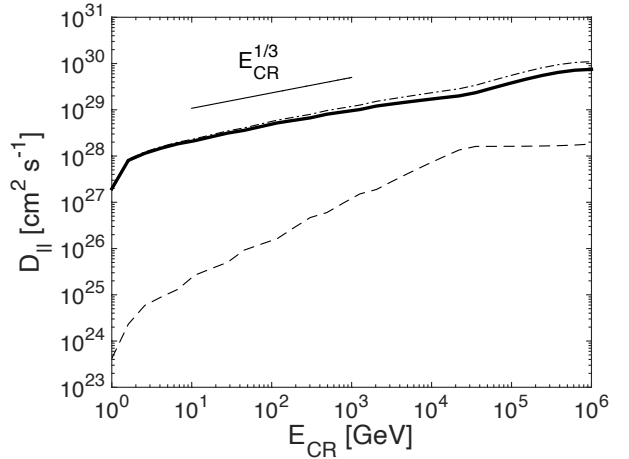
In this work, we introduce a new diffusion mechanism for CRs that encounter magnetic compressions induced by slow (pseudo-Alfvén) and fast modes. This parallel mirror diffusion of CRs can take place even in incompressible MHD turbulence and cause slower diffusion than that induced by scattering in both incompressible and compressible MHD turbulence. In the idealized situation with incompressible turbulence and the streaming instability suppressed by Alfvénic turbulence, bouncing CRs can stay in the system for an extended period of time until they become non-bouncing CRs due to scattering or acceleration processes. This finding has important implications for CR diffusion in high- $\beta$  intracluster media. In addition, the slow diffusion of bouncing CRs near CR sources may provide a possible explanation for the small diffusion coefficient of high-energy electrons and positrons around pulsar wind nebulae suggested by recent observations (e.g., Abeyssekara et al. 2017; Huang et al. 2018), as well as the steep high-energy CR spectra indicated by gamma-ray observations of middle-aged supernova remnants (Xu 2021; see also, e.g., Nava et al. 2016; D’Angelo et al. 2016, 2018; Nava et al. 2019, for suppressed diffusion of self-confined CRs around Galactic sources).

In addition, the mirroring of CRs also affects the parallel diffusion associated with scattering. In the presence of mirroring, the scattering even in the quasilinear approximation does not face the  $90^\circ$  problem (Noerdlinger 1968; Kulsrud & Pearce 1969; Felice & Kulsrud 2001), and also the resulting mean free path corresponds to the pitch angle change over a smaller range  $[\mu_c, 1]$ , as pointed out by Cesarsky & Kulsrud (1973). In XL20, we derived the parallel diffusion coefficient for scattering by fast modes in the presence of bouncing. With an energy-dependent  $\mu_c$ , the diffusion coefficient has a energy dependence close to  $\propto E^{1/3}$  instead of  $\propto E^{0.5}$ . In earlier studies (e.g., Ptuskin et al. 2006), the energy dependence  $\propto E^{1/3}$  of diffusion coefficient is only expected for the Kolmogorov spectrum of turbulence, but the Alfvén and slow modes with the Kolmogorov spectrum are incapable of scattering. Our finding provides a possible solution to this theoretical problem and a possible explanation for the energy scaling of diffusion coefficient of high-energy CRs indicated by observations (e.g., Blasi et al. 2012; Fornieri et al. 2021).

### 6.2. Mirroring and acceleration

The mirroring of CRs also induces a new acceleration mechanism. The mirroring does not change a particle’s pitch angle if the magnetic mirrors are static. When encountering moving magnetic mirrors in MHD turbulence, CRs undergo the second order Fermi acceleration with the stochastic increase of parallel momentum  $p_{\parallel}$  and  $\mu$ . Together with other acceleration mechanisms, e.g., TTD that also causes the stochastic increase of  $\mu$  (Section 6.4), the mirroring can enhance the diffusion in  $\mu$  and the transition of particles from bouncing to non-bouncing state. This new acceleration mechanism and its implications will be studied in our future work.

The diffusive propagation of CRs plays an important role in the first order Fermi acceleration processes at shocks

(a)  $\delta B_f/B_0 = 0, N_s = 0.5$ (b)  $\delta B_f/B_0 = 0.01, N_s = 0.5$ (c)  $\delta B_f/B_0 = 0.1, N_s = 0.5$ (d)  $\delta B_f/B_0 = 0.5, N_s = 0.5$ 

**Figure 7.** Parallel diffusion coefficients of bouncing particles  $D_{\parallel,b}$ , non-bouncing particles  $D_{\parallel,nb}$ , and the averaged parallel diffusion coefficient  $D_{\parallel,tot}$  in MHD turbulence with different fractions of fast modes. The pitch angle distribution is assumed to be isotropic.

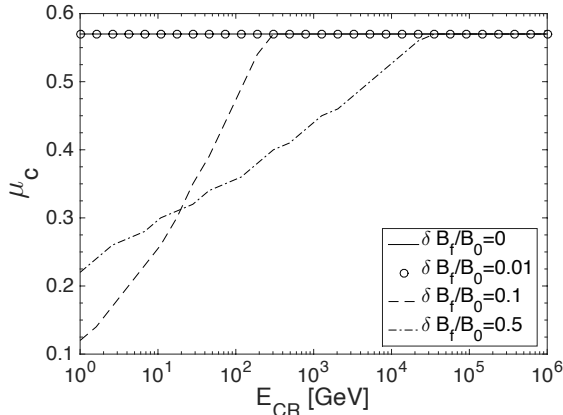


**Figure 8.**  $\mu_c$  vs.  $E_{CR}$  for different fractions of fast modes.

(e.g., Schlickeiser & Oppotsch 2017) and in regions of turbulent magnetic reconnection (de Gouveia dal Pino & Lazarian 2005; Lazarian 2005; Kowal et al. 2012). Both the perpendicular superdiffusion and the parallel diffusion resulting from mirroring and scattering should be taken into account when studying the acceleration of CRs.

### 6.3. Mirroring and instabilities

Mirroring and resonant scattering by MHD turbulence are not the only processes that affect the diffusion of CRs. The fluid of low-energy CRs is subject to instabilities. The streaming instability is the most studied one (Kulsrud 2005). This instability arises when CRs move preferentially in the same direction. The Alfvénic fluctuations that are induced are different from MHD turbulence. These are resonant waves that effectively scatter CRs and prevent free escape of particles. Streaming instability can be important for explaining the energy scaling of diffusion coefficient of low-energy CRs indicated by AMS-02 measurements (e.g., Fornieri et al. 2021).

Apart from the streaming instability, CRs can face other types of instabilities, the importance of which is less explored. For instance, the compression of CRs by turbulence induces anisotropy in the distribution of CRs in momentum space. This can result in the gyroresonance, mirror, and firehose collisionless instabilities of CRs (Lazarian & Berezhnyak 2006). In addition, the faster escape of non-bouncing particles from the vicinity of CRs source changes the momentum distribution toward having more CRs with  $\mu < \mu_c$ .

This difference in the diffusion coefficients of bouncing and non-bouncing CRs is another source of momentum space anisotropy, which can result in an instability and induce resonant Alfvénic waves. The list above does not exhaust the list of the CR instabilities that can be present in the vicinity of CR sources. For instance the current instability (Bell 2004) was introduced in the context of shock acceleration. It is also expected to be present beyond the shock context.

The instabilities, along with the mirroring, can significantly suppress the diffusion of CRs in the vicinity of their sources. The environmental effects, e.g. ambient turbulence, gas ionization, have different influence on mirroring and the scattering caused by instabilities. We note that the CR streaming instability can be suppressed in galactic disks through both ion-neutral collisional damping (Kulsrud & Pearce 1969; Xu et al. 2016; Krumholz et al. 2020) and the interaction with Alfvénic turbulence (Yan & Lazarian 2002; Farmer & Goldreich 2004; Lazarian 2016). More severe damping of streaming instability is expected at a larger  $M_A$  (Lazarian 2016), while the magnetic compressions that cause mirroring increase with  $M_A$  (Hu, Lazarian, & Xu, in prep). Therefore, the relative importance between streaming instability and mirroring effect on diffusion of low-energy CRs depends on  $M_A$ , which varies in the multi-phase interstellar medium (Lazarian et al. 2018). The comparison between scattering by instabilities and mirroring, as well as their interplay, requires further studies.

### 6.4. Mirroring and TTD

The TTD effect is an important component of CR dynamics (Schlickeiser 2002; Yan & Lazarian 2002; Xu & Lazarian 2018). The TTD interaction arises from magnetic compressions in turbulent media. This is the common feature of TTD and mirroring. Nevertheless, they are two different processes and should be distinguished.

The resonant TTD interaction happens when the parallel phase speed of compressible waves matches the parallel speed of the particle. Such interactions can induce the second order Fermi acceleration of  $p_{\parallel}$ . The resulting stochastic increase of  $\mu$  associated with TTD acceleration should be distinguished from the pitch-angle diffusion due to resonant scattering. In contrast, the mirror diffusion does not require any resonance condition. It can take place even in the limit case of stationary magnetic bottles, i.e.  $V_A \rightarrow 0$ , where stochastic acceleration is not involved. As another difference, mirroring can not happen at small pitch angles in the loss cone, but there is no such constraint for TTD.

In brief, TTD is a stochastic acceleration process with acceleration-induced diffusion in  $\mu$ . Mirror diffusion is a diffusion process in space, which can be accompanied by stochastic acceleration.

### 6.5. Damping effect

Fast modes can be subject to ion-neutral collisional damping in partially ionized interstellar phases (Xu et al. 2015, 2016; Xu & Lazarian 2018) and collisionless damping in galactic halo. The effect of damping of fast modes on scat-

tering of CRs has been addressed in earlier studies, e.g., Yan & Lazarian (2002, 2004); Xu et al. (2016); Xu & Lazarian (2018). The effect of damping on mirroring by fast modes will be addressed in our future work. In the case when fast modes are severely damped, slow modes can dominate the bouncing of CRs (see Sections 4 and 5.2).

## 7. SUMMARY

To achieve a more comprehensive description of CR propagation, different diffusion mechanisms depending on the properties of MHD turbulence should be taken into account. In this work we identify the mirror diffusion as an essential process of CR propagation.

The perpendicular superdiffusion of CRs originates from the superdiffusion of magnetic fields induced by Alfvénic turbulence. This effect makes the trapping of CR within magnetic bottles improbable. Instead, CRs bounce with different magnetic mirrors and move diffusively parallel to the turbulent magnetic field. As a result, both magnetic mirroring and pitch-angle scattering contribute to the parallel diffusion. The former governs the parallel diffusion of CRs at large pitch angles with  $\mu < \mu_c$ , and the latter is dominant at  $\mu > \mu_c$ , where  $\mu_c$  corresponds to the balance between mirroring and scattering. The two diffusion processes interact with each other through exchanging CRs via the pitch angle diffusion.

In the case when fast modes dominate both scattering and mirroring,  $\mu_c$  increases with  $E_{CR}$ . As a result, the diffusion coefficient for scattering by fast modes has a weaker dependence on  $E_{CR}$  compared to the case without mirroring, i.e.,  $\mu_c = 0$ . It is not an exact power law function of  $E_{CR}$ , but can be approximated by  $\propto E_{CR}^{1/3}$ . The scaling  $\propto E_{CR}^{1/3}$  is expected for isotropic turbulence with the Kolmogorov spectrum. However, the scattering by Alfvén and slow modes with the Kolmogorov spectrum is inefficient and the resulting diffusion coefficient depends on  $E_{CR}$  as  $\propto E_{CR}^{-3/2}$  due to

the scale-dependent turbulence anisotropy. Our finding provides the physical justification for the commonly used energy scaling of diffusion coefficient.

With the mirroring of CRs taken into account, the 90° problem of quasilinear gyroresonant scattering can be solved. Moreover, as the mean free path of bouncing CRs is determined by the size of compressive magnetic fluctuations, which cannot exceed the driving scale of turbulence, the corresponding diffusion is slow. The energy scaling of the diffusion coefficient of bouncing CRs depends on the anisotropy of pitch angle distribution and the energy dependence of  $\mu_c$ .

In the vicinity of a CR source, the injected CRs can have an anisotropic pitch angle distribution. Note that the damping of turbulence can also affect the anisotropic distribution. If there are more particles at larger pitch angles, the diffusion of bouncing CRs can be further suppressed.

For the galactic environment with a nearly uniform and isotropic distribution of CRs, the average diffusion coefficient of bouncing and non-bouncing CRs on scales much larger than their mean free paths is usually determined by the diffusion coefficient of the latter, as it is larger than that of bouncing CRs. Its energy scaling can be non-universal, depending on the properties of interstellar turbulence.

## ACKNOWLEDGMENTS

S.X. acknowledges the support for this work provided by NASA through the NASA Hubble Fellowship grant # HST-HF2-51473.001-A awarded by the Space Telescope Science Institute, which is operated by the Association of Universities for Research in Astronomy, Incorporated, under NASA contract NAS5-26555.

*Software:* MATLAB (MATLAB 2018)

## APPENDIX

### A. BASIC SCALINGS OF MHD TURBULENCE

#### A.1. Scalings of incompressible MHD turbulence

MHD turbulence is a major agent determining the dynamics of CRs. The turbulence in magnetized media in typical astrophysical settings is injected at the scale  $L$  with the injection velocity  $V_L$ , and the turbulent energy then cascades down to smaller scales. If the injection happens with  $V_L > V_A$ , where  $V_A$  is the Alfvén speed, this is the case of super-Alfvénic turbulence. If  $V_L < V_A$ , the turbulence is sub-Alfvénic. The ratio  $M_A = V_L/V_A$  is the Alfvén Mach number.  $M_A = 1$  corresponds to the trans-Alfvénic turbulence.

Note that we consider turbulence as a result of energy cascade. Therefore the Alfvén waves excited by CR instabilities, e.g. streaming instabilities (see Farmer & Goldreich 2004), gyro-resonance instabilities (see Lazarian & Beresnyak 2006), are not classified as turbulence.

The theory of trans-Alfvénic turbulence was developed by Goldreich & Sridhar (1995) (henceforth GS95) in the global system of reference with respect to the mean magnetic field. Lazarian & Vishniac (1999) (henceforth LV99) presented an alternative way to derive the GS95 theory based on the theory of turbulent reconnection of magnetic fields. More importantly, they found that the GS95 theory is only valid in the “local system of reference” with respect to the local mean magnetic field averaged over the length scale of interest, as confirmed by numerical simulations (Cho & Vishniac 2000; Maron & Goldreich 2001; Cho

et al. 2002). According to the LV99 theory, magnetic reconnection takes place within one eddy turnover time, which allows the turbulent motions to mix up magnetic fields without bending them. The unconstrained eddy rotation occurs in the system of reference of the local magnetic field averaged over the eddy scale, and the eddy is aligned with the local magnetic field. The direction of the local magnetic field averaged over a small scale can differ significantly from the global mean magnetic field direction averaged over a large scale.

The turbulent cascade in the direction perpendicular to the local magnetic field remains Kolmogorov-like with

$$v_l \approx V_A \left( \frac{l_\perp}{L} \right)^{1/3}, \quad (\text{A1})$$

where it is taken into account that  $V_L = V_A$  for trans-Alfvénic turbulence,  $v_l$  is the turbulent velocity at  $l_\perp$ , and  $l_\perp$  is the perpendicular size of a turbulent eddy. The eddy rotation perpendicular to the local magnetic field induces Alfvénic perturbation that propagates along the magnetic field with the speed  $V_A$ . The timescale of this perturbation  $l_\parallel/V_A$  should be equal to the eddy turnover time  $l_\perp/v_l$ . The corresponding relation between the parallel and perpendicular sizes of the eddy

$$\frac{l_\parallel}{V_A} \approx \frac{l_\perp}{v_l}, \quad (\text{A2})$$

was termed as the ‘‘critical balance’’ in GS95. By combining Eq. (A1) and Eq. (A2), one can obtain the scale-dependent anisotropy of trans-Alfvénic turbulence

$$l_\parallel \approx L \left( \frac{l_\perp}{L} \right)^{2/3}. \quad (\text{A3})$$

Smaller eddies are more elongated along the local magnetic field. Note that Eqs. (A1) and (A3) should be understood in the statistical sense. They represent the scaling relations between the most probable values of the quantities involved. For instance, on the basis of numerical simulations, Cho et al. (2002) provided an analytical fit for the detailed distribution function describing the probability of finding a  $l_\perp$  at a given  $l_\parallel$ . This was used later in Yan & Lazarian (2002, 2004) and subsequent studies on CR scattering.

For super-Alfvénic turbulence injected with  $M_A > 1$ , the magnetic field is of marginal importance at  $L$ . The super-Alfvénic turbulence is initially hydrodynamic-like with the isotropic Kolmogorov energy spectrum. With the decrease of turbulent velocity along the energy cascade,  $v_l \sim V_L(l/L)^{1/3}$ , where  $v_l$  is the turbulent velocity at the length scale  $l$ , the effect of magnetic field becomes more and more manifested. Eventually, at the scale (Lazarian 2006)

$$l_A = LM_A^{-3}, \quad (\text{A4})$$

$v_l$  becomes equal to  $V_A$ , and the turbulence becomes fully magnetohydrodynamic. To describe the MHD cascade on scales less than  $l_A$  in super-Alfvénic turbulence,  $L$  in Eqs. (A1) and (A3) should be replaced by  $l_A$ .

For sub-Alfvénic turbulence with  $M_A < 1$ , it was shown in LV99 that at  $L$  the turbulence is *weak*, and the parallel scale of wave packets remains unchanged, i.e.  $l_\parallel = L$ . The scaling obtained in LV99 for the weak turbulence under the assumption of the isotropic turbulence driven at  $L$  is

$$v_l \approx V_L \left( \frac{l_\perp}{L} \right)^{1/2}, \quad (\text{A5})$$

and this result was supported by the subsequent study by Galtier et al. (2000). With the decrease of  $l_\perp$ , the intensity of interactions of Alfvénic perturbations increases. At a scale (LV99)

$$l_{\text{tran}} \approx LM_A^2, \quad (\text{A6})$$

where  $M_A < 1$ , the turbulence gets strong. For the sub-Alfvénic MHD turbulence at  $l < l_{\text{tran}}$ , LV99 derived the relations

$$v_l \approx V_L \left( \frac{l_\perp}{L} \right)^{1/3} M_A^{1/3}, \quad (\text{A7})$$

and

$$l_\parallel \approx L \left( \frac{l_\perp}{L} \right)^{2/3} M_A^{-4/3}, \quad (\text{A8})$$

which at  $M_A = 1$  can recover the relations in Eqs. (A1) and (A3) for trans-Alfvénic turbulence.

To generalize our analysis for diffusion of bouncing particles in trans-Alfvénic turbulence to super- and sub-Alfvénic turbulence, we introduce the following effective injection scales.

(1) Super-Alfvénic turbulence. As discussed above, the super-Alfvénic turbulence at  $l < l_A$  is equivalent to the trans-Alfvénic turbulence injected at  $l_A$ . So by using  $l_A$  as the effective injection scale to replace  $L$  in trans-Alfvénic turbulence, the results derived for trans-Alfvénic are still applicable to super-Alfvénic on scales less than  $l_A$ .

(2) Sub-Alfvénic turbulence. By introducing an effective injection scale

$$L_{\text{eff}} = LM_A^{-4}, \quad (\text{A9})$$

Eqs. (A7) and (A8) can be rewritten as

$$v_l \approx V_A \left( \frac{l_{\perp}}{L_{\text{eff}}} \right)^{1/3}, \quad (\text{A10})$$

and

$$l_{\parallel} \approx L_{\text{eff}} \left( \frac{l_{\perp}}{L_{\text{eff}}} \right)^{2/3}, \quad (\text{A11})$$

which take the same forms as Eqs. (A1) and (A3) with  $L$  replaced by  $L_{\text{eff}}$ . Therefore, by using  $L_{\text{eff}}$  instead of  $L$ , the expressions for trans-Alfvénic turbulence can be applied to sub-Alfvénic turbulence on scales less than  $l_{\text{tran}}$ .

### A.2. Magnetic compressions in MHD turbulence

The magnetic mirroring effect arise from the magnetic compressions in MHD turbulence, which are associated with slow and fast modes. We use the term “modes” rather than “waves”, as the nonlinear interactions intrinsic to the turbulent cascade make the properties of magnetic fluctuations different from the properties of linear waves. We stress that the compression of magnetic field can also occur in incompressible MHD turbulence. The incompressible limit of slow modes, i.e., pseudo-Alfvén modes (see GS95), is a typical example for turbulent compression of magnetic field in an incompressible medium.

It was pointed out in GS95 that Alfvén modes impose their scaling on the pseudo-Alfvén modes. With a finite compressibility, slow modes also follow the same scaling as Alfvén modes. This property was discussed in Lithwick & Goldreich (2001) and confirmed numerically by Cho & Lazarian (2002b, 2003). As discussed above, the anisotropic scaling of slow modes is defined and should be measured in the local system of reference. For bouncing CRs that interact with the magnetic compression generated by slow modes, they only feel the local magnetic field averaged over the scale of the magnetic compression. When describing the gyroresonant scattering of non-bouncing CRs, they also only feel the local magnetic field averaged over the scale comparable to  $r_L$ . The QLT for scattering is formally only applicable to infinitesimally small magnetic perturbations. In the local system of reference, CRs only interact with the small magnetic fluctuations on small scales, while the large fluctuations on large scales are not involved. This extends the applicability of the QLT.

Fast modes are different from Alfvén and slow modes. Their evolution is not related to the local system of reference. Therefore, the traditional wave representation is applicable to fast modes. The scaling of fast modes is somewhat less certain. The theoretical considerations in LG01 for high- $\beta$  plasma and in Cho & Lazarian (2002b, 2003) for low- $\beta$  plasma suggested the “isotropic” energy spectrum of fast modes with  $k^{-3/2}$  similar to the acoustic-type turbulence. However, the simulations in Kowal & Lazarian (2010) indicated a steeper spectrum close to  $k^{-2}$  for fast modes. This discrepancy may be attributed to the effect of shocks in the latter study.

## REFERENCES

- Abeysekara, A. U., Albert, A., Alfaro, R., et al. 2017, *Science*, 358, 911, doi: [10.1126/science.aan4880](https://doi.org/10.1126/science.aan4880)
- Amato, E., & Casanova, S. 2021, *Journal of Plasma Physics*, 87, 845870101, doi: [10.1017/S0022377821000064](https://doi.org/10.1017/S0022377821000064)
- Bell, A. R. 2004, *MNRAS*, 353, 550, doi: [10.1111/j.1365-2966.2004.08097.x](https://doi.org/10.1111/j.1365-2966.2004.08097.x)
- Beresnyak, A. 2013, *ApJL*, 767, L39, doi: [10.1088/2041-8205/767/2/L39](https://doi.org/10.1088/2041-8205/767/2/L39)
- . 2014, *ApJL*, 784, L20, doi: [10.1088/2041-8205/784/2/L20](https://doi.org/10.1088/2041-8205/784/2/L20)
- Beresnyak, A., & Lazarian, A. 2019, *Turbulence in Magnetohydrodynamics*
- Blasi, P., Amato, E., & Serpico, P. D. 2012, *PhRvL*, 109, 061101, doi: [10.1103/PhysRevLett.109.061101](https://doi.org/10.1103/PhysRevLett.109.061101)
- Brunetti, G., & Jones, T. W. 2014, *International Journal of Modern Physics D*, 23, 1430007, doi: [10.1142/S0218271814300079](https://doi.org/10.1142/S0218271814300079)
- Brunetti, G., & Lazarian, A. 2007, *MNRAS*, 378, 245, doi: [10.1111/j.1365-2966.2007.11771.x](https://doi.org/10.1111/j.1365-2966.2007.11771.x)
- Budker, G. I. 1959, in *Plasma Physics and the Problem of Controlled Thermonuclear Reactions*, Ed. by M. A. Leontovich (Pergamon, New York), Vol. 1
- Cesarsky, C. J., & Kulsrud, R. M. 1973, *ApJ*, 185, 153
- Chandran, B. D. G. 2000a, *Physical Review Letters*, 85, 4656, doi: [10.1103/PhysRevLett.85.4656](https://doi.org/10.1103/PhysRevLett.85.4656)

- Chandran, B. D. G. 2000b, *ApJ*, 529, 513, doi: [10.1086/308232](https://doi.org/10.1086/308232)
- Chepurnov, A., Lazarian, A., Stanimirović, S., Heiles, C., & Peek, J. E. G. 2010, *ApJ*, 714, 1398, doi: [10.1088/0004-637X/714/2/1398](https://doi.org/10.1088/0004-637X/714/2/1398)
- Cho, J., & Lazarian, A. 2002a, *ApJL*, 575, L63, doi: [10.1086/342722](https://doi.org/10.1086/342722)
- . 2002b, *Physical Review Letters*, 88, 245001, doi: [10.1103/PhysRevLett.88.245001](https://doi.org/10.1103/PhysRevLett.88.245001)
- . 2003, *MNRAS*, 345, 325, doi: [10.1046/j.1365-8711.2003.06941.x](https://doi.org/10.1046/j.1365-8711.2003.06941.x)
- Cho, J., Lazarian, A., & Timbie, P. T. 2012, *ApJ*, 749, 164, doi: [10.1088/0004-637X/749/2/164](https://doi.org/10.1088/0004-637X/749/2/164)
- Cho, J., Lazarian, A., & Vishniac, E. T. 2002, *ApJ*, 564, 291, doi: [10.1086/324186](https://doi.org/10.1086/324186)
- Cho, J., & Vishniac, E. T. 2000, *ApJ*, 539, 273, doi: [10.1086/309213](https://doi.org/10.1086/309213)
- Cohet, R., & Marcowith, A. 2016, *A&A*, 588, A73, doi: [10.1051/0004-6361/201527376](https://doi.org/10.1051/0004-6361/201527376)
- D'Angelo, M., Blasi, P., & Amato, E. 2016, *PhRvD*, 94, 083003, doi: [10.1103/PhysRevD.94.083003](https://doi.org/10.1103/PhysRevD.94.083003)
- D'Angelo, M., Morlino, G., Amato, E., & Blasi, P. 2018, *MNRAS*, 474, 1944, doi: [10.1093/mnras/stx2828](https://doi.org/10.1093/mnras/stx2828)
- de Gouveia dal Pino, E. M., & Lazarian, A. 2005, *A&A*, 441, 845, doi: [10.1051/0004-6361:20042590](https://doi.org/10.1051/0004-6361:20042590)
- Demidem, C., Lemoine, M., & Casse, F. 2020, *PhRvD*, 102, 023003, doi: [10.1103/PhysRevD.102.023003](https://doi.org/10.1103/PhysRevD.102.023003)
- Evoli, C., & Yan, H. 2014, *ApJ*, 782, 36, doi: [10.1088/0004-637X/782/1/36](https://doi.org/10.1088/0004-637X/782/1/36)
- Eyink, G., Vishniac, E., Lalescu, C., et al. 2013, *Nature*, 497, 466, doi: [10.1038/nature12128](https://doi.org/10.1038/nature12128)
- Eyink, G. L., Lazarian, A., & Vishniac, E. T. 2011, *ApJ*, 743, 51, doi: [10.1088/0004-637X/743/1/51](https://doi.org/10.1088/0004-637X/743/1/51)
- Farmer, A. J., & Goldreich, P. 2004, *ApJ*, 604, 671, doi: [10.1086/382040](https://doi.org/10.1086/382040)
- Felice, G. M., & Kulsrud, R. M. 2001, *ApJ*, 553, 198, doi: [10.1086/320651](https://doi.org/10.1086/320651)
- Fermi, E. 1949, *Physical Review*, 75, 1169, doi: [10.1103/PhysRev.75.1169](https://doi.org/10.1103/PhysRev.75.1169)
- Fisk, L. A., Goldstein, M. L., Klimas, A. J., & Sandri, G. 1974, *ApJ*, 190, 417, doi: [10.1086/152893](https://doi.org/10.1086/152893)
- Forman, M. A., Wicks, R. T., & Horbury, T. S. 2011, *ApJ*, 733, 76, doi: [10.1088/0004-637X/733/2/76](https://doi.org/10.1088/0004-637X/733/2/76)
- Fornieri, O., Gaggero, D., Cerri, S. S., De La Torre Luque, P., & Gabici, S. 2021, *MNRAS*, 502, 5821, doi: [10.1093/mnras/stab355](https://doi.org/10.1093/mnras/stab355)
- Gabici, S., Evoli, C., Gaggero, D., et al. 2019, arXiv e-prints, arXiv:1903.11584. <https://arxiv.org/abs/1903.11584>
- Galtier, S., Nazarenko, S. V., Newell, A. C., & Pouquet, A. 2000, *Journal of Plasma Physics*, 63, 447, doi: [10.1017/S0022377899008284](https://doi.org/10.1017/S0022377899008284)
- Giacalone, J., & Jokipii, J. R. 1999, *ApJ*, 520, 204, doi: [10.1086/307452](https://doi.org/10.1086/307452)
- Goldreich, P., & Sridhar, S. 1995, *ApJ*, 438, 763, doi: [10.1086/175121](https://doi.org/10.1086/175121)
- Guo, F., & Oh, S. P. 2008, *MNRAS*, 384, 251, doi: [10.1111/j.1365-2966.2007.12692.x](https://doi.org/10.1111/j.1365-2966.2007.12692.x)
- Holguin, F., Ruszkowski, M., Lazarian, A., Farber, R., & Yang, H. Y. K. 2019, *MNRAS*, 490, 1271, doi: [10.1093/mnras/stz2568](https://doi.org/10.1093/mnras/stz2568)
- Horbury, T. S., Forman, M., & Oughton, S. 2008, *PhRvL*, 101, 175005, doi: [10.1103/PhysRevLett.101.175005](https://doi.org/10.1103/PhysRevLett.101.175005)
- Huang, Z.-Q., Fang, K., Liu, R.-Y., & Wang, X.-Y. 2018, *ApJ*, 866, 143, doi: [10.3847/1538-4357/aadfed](https://doi.org/10.3847/1538-4357/aadfed)
- Ipavich, F. M. 1975, *ApJ*, 196, 107, doi: [10.1086/153397](https://doi.org/10.1086/153397)
- Jokipii, J. R. 1966, *ApJ*, 146, 480, doi: [10.1086/148912](https://doi.org/10.1086/148912)
- . 1971, *Reviews of Geophysics and Space Physics*, 9, 27, doi: [10.1029/RG009i001p00027](https://doi.org/10.1029/RG009i001p00027)
- Klepach, E. G., & Ptuskin, V. S. 1995, *Astronomy Letters*, 21, 411
- Kóta, J., & Jokipii, J. R. 2000, *ApJ*, 531, 1067, doi: [10.1086/308492](https://doi.org/10.1086/308492)
- Kowal, G., de Gouveia Dal Pino, E. M., & Lazarian, A. 2012, *Physical Review Letters*, 108, 241102, doi: [10.1103/PhysRevLett.108.241102](https://doi.org/10.1103/PhysRevLett.108.241102)
- Kowal, G., Falceta-Gonçalves, D. A., Lazarian, A., & Vishniac, E. T. 2017, *ApJ*, 838, 91, doi: [10.3847/1538-4357/aa6001](https://doi.org/10.3847/1538-4357/aa6001)
- Kowal, G., & Lazarian, A. 2010, *ApJ*, 720, 742, doi: [10.1088/0004-637X/720/1/742](https://doi.org/10.1088/0004-637X/720/1/742)
- Kowal, G., Lazarian, A., Vishniac, E. T., & Otmianowska-Mazur, K. 2009, in *Revista Mexicana de Astronomía y Astrofísica Conference Series*, Vol. 36, *Revista Mexicana de Astronomía y Astrofísica Conference Series*, 89–96. <https://arxiv.org/abs/0812.2024>
- Krumholz, M. R., Crocker, R. M., Xu, S., et al. 2020, *MNRAS*, 493, 2817, doi: [10.1093/mnras/staa493](https://doi.org/10.1093/mnras/staa493)
- Kulsrud, R., & Pearce, W. P. 1969, *ApJ*, 156, 445, doi: [10.1086/149981](https://doi.org/10.1086/149981)
- Kulsrud, R. M. 2005, *Plasma physics for astrophysics*, ed. R. M. Kulsrud
- Lazarian, A. 2005, in *American Institute of Physics Conference Series*, Vol. 784, *Magnetic Fields in the Universe: From Laboratory and Stars to Primordial Structures.*, ed. E. M. de Gouveia dal Pino, G. Lugones, & A. Lazarian, 42–53, doi: [10.1063/1.2077170](https://doi.org/10.1063/1.2077170)
- Lazarian, A. 2006, *ApJL*, 645, L25, doi: [10.1086/505796](https://doi.org/10.1086/505796)
- . 2016, *ApJ*, 833, 131, doi: [10.3847/1538-4357/833/2/131](https://doi.org/10.3847/1538-4357/833/2/131)
- Lazarian, A., & Beresnyak, A. 2006, *MNRAS*, 373, 1195, doi: [10.1111/j.1365-2966.2006.11093.x](https://doi.org/10.1111/j.1365-2966.2006.11093.x)
- Lazarian, A., & Vishniac, E. T. 1999, *ApJ*, 517, 700, doi: [10.1086/307233](https://doi.org/10.1086/307233)
- Lazarian, A., Vishniac, E. T., & Cho, J. 2004, *ApJ*, 603, 180, doi: [10.1086/381383](https://doi.org/10.1086/381383)

- Lazarian, A., & Yan, H. 2014, *ApJ*, 784, 38,  
doi: [10.1088/0004-637X/784/1/38](https://doi.org/10.1088/0004-637X/784/1/38)
- . 2019, *ApJ*, 885, 170, doi: [10.3847/1538-4357/ab50ba](https://doi.org/10.3847/1538-4357/ab50ba)
- Lazarian, A., Yuen, K. H., Ho, K. W., et al. 2018, *ApJ*, 865, 46,  
doi: [10.3847/1538-4357/aad7ff](https://doi.org/10.3847/1538-4357/aad7ff)
- Lemoine, M., & Malkov, M. A. 2020, *MNRAS*, 499, 4972,  
doi: [10.1093/mnras/staa3131](https://doi.org/10.1093/mnras/staa3131)
- Lithwick, Y., & Goldreich, P. 2001, *ApJ*, 562, 279,  
doi: [10.1086/323470](https://doi.org/10.1086/323470)
- López-Barquero, V., Farber, R., Xu, S., Desiati, P., & Lazarian, A. 2016, *ApJ*, 830, 19, doi: [10.3847/0004-637X/830/1/19](https://doi.org/10.3847/0004-637X/830/1/19)
- Luo, Q. Y., & Wu, D. J. 2010, *ApJL*, 714, L138,  
doi: [10.1088/2041-8205/714/1/L138](https://doi.org/10.1088/2041-8205/714/1/L138)
- Lynn, J. W., Parrish, I. J., Quataert, E., & Chandran, B. D. G. 2012, *ApJ*, 758, 78, doi: [10.1088/0004-637X/758/2/78](https://doi.org/10.1088/0004-637X/758/2/78)
- Maron, J., & Goldreich, P. 2001, *ApJ*, 554, 1175,  
doi: [10.1086/321413](https://doi.org/10.1086/321413)
- MATLAB. 2018, 9.7.0.1190202 (R2019b) (Natick, Massachusetts: The MathWorks Inc.)
- Matthaeus, W. H., Goldstein, M. L., & Roberts, D. A. 1990, *J. Geophys. Res.*, 95, 20673, doi: [10.1029/JA095iA12p20673](https://doi.org/10.1029/JA095iA12p20673)
- Matthaeus, W. H., Qin, G., Bieber, J. W., & Zank, G. P. 2003, *ApJL*, 590, L53, doi: [10.1086/376613](https://doi.org/10.1086/376613)
- Nava, L., & Gabici, S. 2013, *MNRAS*, 429, 1643,  
doi: [10.1093/mnras/sts450](https://doi.org/10.1093/mnras/sts450)
- Nava, L., Gabici, S., Marcowith, A., Morlino, G., & Ptuskin, V. S. 2016, *MNRAS*, 461, 3552, doi: [10.1093/mnras/stw1592](https://doi.org/10.1093/mnras/stw1592)
- Nava, L., Recchia, S., Gabici, S., et al. 2019, *MNRAS*, 484, 2684,  
doi: [10.1093/mnras/stz137](https://doi.org/10.1093/mnras/stz137)
- Noerdlinger, P. D. 1968, *PhRvL*, 20, 1513,  
doi: [10.1103/PhysRevLett.20.1513](https://doi.org/10.1103/PhysRevLett.20.1513)
- Orlando, E. 2018, *MNRAS*, 475, 2724,  
doi: [10.1093/mnras/stx3280](https://doi.org/10.1093/mnras/stx3280)
- Padovani, M., Ivlev, A. V., Galli, D., & Caselli, P. 2018, *A&A*, 614, A111, doi: [10.1051/0004-6361/201732202](https://doi.org/10.1051/0004-6361/201732202)
- Palmer, I. D. 1982, *Reviews of Geophysics and Space Physics*, 20, 335, doi: [10.1029/RG020i002p00335](https://doi.org/10.1029/RG020i002p00335)
- Parker, E. N. 1965, *Planet. Space Sci.*, 13, 9,  
doi: [10.1016/0032-0633\(65\)90131-5](https://doi.org/10.1016/0032-0633(65)90131-5)
- Post, R. F. 1958, *Proc. of Second U.N. Int. Conf. on Peaceful Uses of Atomic Energy*, Vol. 32, Paper A/Conf. 15/P/377, Geneva, pp. 245-265
- Ptuskin, V. S., Moskalenko, I. V., Jones, F. C., Strong, A. W., & Zirakashvili, V. N. 2006, *ApJ*, 642, 902, doi: [10.1086/501117](https://doi.org/10.1086/501117)
- Qin, G., Matthaeus, W. H., & Bieber, J. W. 2002, *ApJL*, 578, L117,  
doi: [10.1086/344687](https://doi.org/10.1086/344687)
- Richardson, L. F. 1926, *Proceedings of the Royal Society of London Series A*, 110, 709, doi: [10.1098/rspa.1926.0043](https://doi.org/10.1098/rspa.1926.0043)
- Schlickeiser, R. 2002, *Cosmic Ray Astrophysics*, ed. R. Schlickeiser
- Schlickeiser, R., Caglar, M., & Lazarian, A. 2016, *ApJ*, 824, 89,  
doi: [10.3847/0004-637X/824/2/89](https://doi.org/10.3847/0004-637X/824/2/89)
- Schlickeiser, R., & Miller, J. A. 1998, *ApJ*, 492, 352,  
doi: [10.1086/305023](https://doi.org/10.1086/305023)
- Schlickeiser, R., & Oppotsch, J. 2017, *ApJ*, 850, 160,  
doi: [10.3847/1538-4357/aa970e](https://doi.org/10.3847/1538-4357/aa970e)
- Singer, H. J., Heckman, G. R., & Hirman, J. W. 2001, *Washington DC American Geophysical Union Geophysical Monograph Series*, 125, 23, doi: [10.1029/GM125p0023](https://doi.org/10.1029/GM125p0023)
- Sioulas, N., Isliker, H., Vlahos, L., Koumtzis, A., & Pisokas, T. 2020, *MNRAS*, 491, 3860, doi: [10.1093/mnras/stz3259](https://doi.org/10.1093/mnras/stz3259)
- Voelk, H. J. 1975, *Reviews of Geophysics and Space Physics*, 13, 547, doi: [10.1029/RG013i004p00547](https://doi.org/10.1029/RG013i004p00547)
- Xu, S. 2021, submitted
- Xu, S., & Lazarian, A. 2018, *ApJ*, 868, 36,  
doi: [10.3847/1538-4357/aae840](https://doi.org/10.3847/1538-4357/aae840)
- . 2020, *ApJ*, 894, 63, doi: [10.3847/1538-4357/ab8465](https://doi.org/10.3847/1538-4357/ab8465)
- Xu, S., Lazarian, A., & Yan, H. 2015, *ApJ*, 810, 44,  
doi: [10.1088/0004-637X/810/1/44](https://doi.org/10.1088/0004-637X/810/1/44)
- Xu, S., & Yan, H. 2013, *ApJ*, 779, 140,  
doi: [10.1088/0004-637X/779/2/140](https://doi.org/10.1088/0004-637X/779/2/140)
- Xu, S., Yan, H., & Lazarian, A. 2016, *ApJ*, 826, 166,  
doi: [10.3847/0004-637X/826/2/166](https://doi.org/10.3847/0004-637X/826/2/166)
- Yan, H., & Lazarian, A. 2002, *Physical Review Letters*, 89, B1102+, doi: [10.1103/PhysRevLett.89.281102](https://doi.org/10.1103/PhysRevLett.89.281102)
- . 2003, *ApJL*, 592, L33, doi: [10.1086/377487](https://doi.org/10.1086/377487)
- . 2004, *ApJ*, 614, 757, doi: [10.1086/423733](https://doi.org/10.1086/423733)
- . 2008, *ApJ*, 673, 942, doi: [10.1086/524771](https://doi.org/10.1086/524771)